# Neuronal PAS domain protein 4 (Npas4) controls neuronal homeostasis in pentylenetetrazole-induced epilepsy through the induction of Homer1a

**Running title:** Npas4-homer1a pathway controls epilepsy

Wei Shan[1,#], Taku Nagai[1,#,*], Motoki Tanaka[2,#], Norimichi Itoh[1], Yoko Furukawa-Hibi[1], Toshitaka Nabeshima[3,4], Masahiro Sokabe[2], Kiyofumi Yamada[1,*]

[1]Department of Neuropsychopharmacology and Hospital Pharmacy, Nagoya University Graduate School of Medicine, Nagoya 466-8560, Japan.

[2]Mechanobiology Laboratory, Nagoya University Graduate School of Medicine, Nagoya 466-8550, Japan.

[3]Advanced Diagnostic System Research Laboratory, Graduate School of Health Sciences, Fujita Health University, Toyoake 470-1192, Japan.

[4]Aino University, Ibaragi 567-0012, Japan.

[*] Corresponding Author.

[#]Co-first author.

*Corresponding Author: Kiyofumi Yamada (kyamada@med.nagoya-u.ac.jp) and Taku Nagai (t-nagai@med.nagoya-u.ac.jp), Department of Neuropsychopharmacology and Hospital Pharmacy, Nagoya University Graduate School of Medicine, 65 Tsurumai-cho, Showa-ku, Nagoya 466-8560, Japan.

**Keywords:** Npas4, epilepsy, homeostasis, synaptic scaling, transcription factor.

**Abbreviations**

AAV, adeno-associated virus; AC, associational/commissural fiber; ACSF, artificial cerebrospinal fluid; AMPAR, α-amino-3-hydroxy-5-methyl-4-isoxazole propionic acid-type glutamate receptor; ANOVA, analysis of variance; BDNF, brain-derived neurotrophic factor; ChIP, chromatin immunoprecipitation; CREB, CRE-binding protein; fEPSPs, field excitatory postsynaptic potentials; FISH, fluorescence *in situ* hybridization; GFAP, glial fibrillary acidic protein; IP3, inositol-1,4,5-triphosphate; mGluR, metabotropic glutamate receptor; mEPSCs, miniature excitatory postsynaptic currents; MF, mossy fiber; NeuN, neuronal nuclei; Npas4, neuronal PAS domain protein 4; PFA, paraformaldehyde; PSD, postsynaptic density protein; PSFV, presynaptic fiber volley; PTZ, pentylenetetrazol; TTX, tetrodotoxin.

**Conflict of interest:** The authors declare no competing financial interests.

**Abstract**

Neuronal intrinsic homeostatic scaling-down of excitatory synapse has been implicated in epilepsy pathogenesis to prevent the neuronal circuits from hyper-excitability. Recent findings suggest a role for neuronal PAS domain protein 4 (Npas4), an activity-dependent neuron-specific transcription factor in epileptogenesis, however, the underlying mechanism by which Npas4 regulates epilepsy remains unclear. We herein propose that limbic seizure activity up-regulates Npas4-homer1a signaling in the hippocampus, thereby contributing to epileptogenesis in mice. The expression level of *Npas4* mRNA was significantly increased after the pentylenetetrazol (PTZ) treatment. *Npas4* KO mice developed kindling more rapidly than their wild-type littermates. The expression of Homer1a in the hippocampus increased after seizure activity. Npas4 increased Homer1a promotor activity in COS7 cells. The PTZ-stimulated induction of Homer1a was attenuated in the hippocampus of *Npas4* KO mice. The combination of fluorescence in situ hybridization and immunohistochemical analyses revealed that *Homer1a* mRNA co-localized with the Npas4 protein after the convulsive seizure response. PTZ reduced excitatory synaptic transmission at the associational/commissural fibers-CA3 synapses through the Npas4-mediated down-regulation of postsynaptic α-amino-3-hydroxy-5-methyl-4-isoxazolepropionic acid receptors (AMPARs) in hippocampal CA3 neurons. The AAV-mediated expression of Homer1a resulted in lower AMPAR GluA1 subunit levels in the hippocampal plasma membrane fraction than in that from AAV-EGFP-transfected *Npas4* KO mice. The development of kindling was more strongly suppressed in AAV-Homer1a-microinjected *Npas4* KO mice than in AAV-EGFP-microinjected *Npas4* KO mice. These results indicate that Npas4 functions as a

molecular switch to initiate homeostatic scaling and the targeting of Npas4-Homer1a signaling may provide new approaches for the treatment of epilepsy.

## Introduction

Epilepsy is a common and refractory neurological disorder (Bell *et al.* 2014). Current anti-epileptic drugs function by symptomatically suppressing seizures once they occur (Loscher *et al.* 2013), and primarily enhance the threshold for seizures without a significant anti-epileptogenic effect (Galanopoulou *et al.* 2012). Furthermore, approximately 20% of epileptic patients continue to have seizures even though they are receiving pharmacological treatment (Kwan *et al.* 2011). The key to preventing and curing epilepsy is to elucidate the mechanisms underlying epileptogenesis.

Previous studies indicated that multiple factors, such as lipoprotein receptor-related protein 4 (Sun *et al.* 2016), sonic hedgehog (Feng *et al.* 2016), brain-derived neurotrophic factor (BDNF) (Liu *et al.* 2013, Gu *et al.* 2015, Mizoguchi *et al.* 2011), and neuregulin 1 (Tan *et al.* 2011, Li *et al.* 2011), are may be involved in epileptogenesis because they may affect the balance between excitatory and inhibitory neurons, leading to neuronal hyperexcitability and recurrent seizures (Turrigiano 2011). However, our understanding of the cellular and molecular mechanisms responsible for epileptogenesis remains incomplete. An alternative and plausible explanation for epileptogenesis is underlying neuronal intrinsic homeostasis during epilepsy which refers to the scaling process by which neurons regulate their excitability (Staley 2015, O'Leary and Wyllie 2011), such as activity-induced Polo-like kinase 2 (Seeburg and Sheng 2008) and accumulation of postsynaptic density protein (PSD)-93/95 (Sun and Turrigiano 2011). Previous studies reported that the homeostatic regulation of synaptic strength was controlled by the surface expression of the α-amino-3-hydroxy-5-methyl-4-isoxazolepropionic acid receptor (AMPAR) (Turrigiano 2008, Seeburg and Sheng 2008, Sun and Turrigiano 2011, Hu *et al.* 2010). Synaptic AMPAR

accumulation in rat cultured cortical neurons was rapidly increased or decreased within 4 h following bath application of voltage-gated sodium channel blocker tetrodotoxin (TTX) or $GABA_A$ receptor antagonist bicucullin, respectively, and the synaptic scaling was maintained for up to 24 h (Ibata *et al.* 2008), suggesting that transcriptional control is involved in synaptic scaling.

Neuronal PAS domain protein 4 (Npas4), a neuron-specific transcriptional factor, is critical for the activity-dependent regulation of GABAergic synapse development *in vitro* though affecting the expression of BDNF (Lin *et al.* 2008). The expression of Npas4 is rapidly activated by excitatory synaptic activity and turns on a program of gene expression that triggers the formation and/or maintenance of inhibitory synapses on excitatory neurons (Spiegel *et al.* 2014). In the regulation and maintenance of normal brain functioning, the induction of Npas4 appears to directly control activity-dependent gene expression, and regulates long-lasting brain function such as memory formation, adaptation, and synaptic plasticity (Lin *et al.* 2008, Ramamoorthi *et al.* 2011, Sun and Lin 2016, Sim *et al.* 2013, Ye *et al.* 2016, Yun *et al.* 2010).

In the present study, we showed that activation of the Npas4 signaling pathway after convulsive seizures plays a crucial role in intrinsic homeostatic scaling during epileptogenesis using an animal model of epilepsy, pentylenetetrazol (PTZ)-induced kindling. Furthermore, we found that Npas4 controlled the homeostatic scaling capacity of hippocampal neurons through the introduction of Homer1a, which regulates the surface expression of the AMPAR GluA1 subunit. Our results provide a molecular link between excessive neuronal hyperexcitability and the regulation of homeostatic scaling for controlling epilepsy.

## Materials and Methods

### Animals

Eight-week-old male C57BL/6 mice (RRID:IMSR_JAX:000664) were purchased from Japan SLC (Hamamatsu, Japan). *Npas4* KO mice (RRID:MGI:3828102) on a C57BL/6 genetic background were kindly provided by Dr. Michael E. Greenberg (Harvard Medical School, Boston, MA, USA) and has been previously described (Lin *et al.* 2008). Mice were housed in a density of five mice per cage (28 cm length × 17 cm width ×13 cm high) under standard conditions (23±1°C, 50±5% humidity) with a 12-h light/dark cycle. Food and water were available ad libitum. This study was approved by the Institutional Animal Care and Use Committee of Nagoya University (approved number 29201). This study was not pre-registered. Animals were handled in accordance with the guidelines established by the Institutional Animal Care and Use Committee of Nagoya University. The male mice used in this study were 8-16 weeks old and 22-29 g body weight unless otherwise indicated. We excluded 3 mice because of abnormal growth (e.g. low body weight less than 20 g at the age of 8 weeks old) in the present study. We measured body weight gain in each mouse before the PTZ or saline treatment to minimize animals' suffering during experiments. Time-line of each experimental schedule was shown in each figure and described in each result. When neurochemical experiments were carried out, mice were decapitated under deep anesthesia with tribromoethanol (200 mg/kg, i.p.) or a combination anesthetic agent (i.p.) containing 0.15 mg/kg medetomidine, 2 mg/kg midazolam, and 2.5 mg/kg butorphanol to reduce animal pain.

**PTZ-induced seizure model and seizure scoring**

PTZ (Sigma, St. Louis, MO, USA) was dissolved in sterile saline. Wild-type and *Npas4* KO mice were randomly assigned into saline or PTZ groups by simple or permuted block method using a completely randomized digital table created in Microsoft Excel (Redmond, DC, USA). Observers were blinded to the grouping and experimental design during data collection and analysis. Behavioal experiment was carred out during 10:00-17:00. Mice were administered 45 mg/kg (i.p.) for the acute seizure model, and 25 mg/kg every 48 h for the kindling model. Mice were immediately placed in a chamber (32 cm length × 21 cm width ×13 cm high) and seizure levels were scored for 20 min. Mice showing more than three consecutive stage 4 seizure levels were defined as kindled mice. Behavioral responses to PTZ were scored according to previous studies (Ferraro *et al.* 1999): stage 0, no response; stage 1, ear and facial twitching; stage 2, convulsive waves through the body; stage 3, myoclonic jerks, stage 4, clonic-tonic convulsions, turnover in the side position; stage 5, generalized clonic-tonic epileptics, loss of postural control; stage 6, death.

**RNA extraction and real-time RT-PCR**

Hippocampal tissues were quickly dissected out on ice and total RNA was extracted using the RNeasy Mini Kit (Qiagen, Hilden, Germany). Total RNA was reverse transcribed using the PrimeScript RT Reagent Kit (Takara Bio, Kusatsu, Japan). Level of Npas4 mRNA were determined after reverse transcription by real-time PCR using an ABI PRISM 7300 real time PCR system (Thermo Fisher Scientific, Yokohama, Japan). We also assessed *cFos* mRNA expression to monitor neuronal excitation (Erdtmann-Vourliotis *et al.* 1998). The

primers used were as follows: *Npas4* forward, TCAACAGAAGGCGCAAACAC; *Npas4* reverse, TGACAGGTCCTTCACCGTGA; *cFos* forward, AAGTAGTGCAGCCCGGAGTA; *cFos* reverse, CCAGTCAAGAGCATCAGCAA; *Homer1a* forward, GAAGTCGCAGGAGAAGATG; *Homer1a* reverse TGATTGCTGAATTGAATGTGTACC; *Homer1c* forward, ACACCCGATGTGACACAGAACT; *Homer1c* reverse, TCAACCTCCCAGTGGTTGCT; *Gapdh* forward, CAATGTGTCCGTCGTGGATCT; *Gapdh* reverse GTCCTC AGTGTAGCCCAAGATG.

**_In situ_ hybridization**

*In situ* hybridization was performed using the DIG RNA Labeling Kit and DIG Nucleic Acid Detection Kit (Roche, Mannheim, Germany) as described previously (Jiang *et al.* 2004). Briefly, the PCR product from mouse *Npas4* (NM_153553, sequence 945–1903 bp) was inserted into the pSPT18 vector. DIG-labeled antisense or sense RNA probes were prepared from linearized plasmids using an SP6 or T7 RNA polymerase *in vitro* transcription kit (Roche). Frozen mouse brain sections (10 μm) were fixed in 4% paraformaldehyde (PFA), digested with Proteinase K (5 μg/ml), acetylated, and then hybridized with DIG-labeled riboprobes at 50°C overnight. DIG-labeled RNA hybrids were reacted with an AP-conjugated anti-DIG antibody (Roche, RRID:AB_514497) at 4°C overnight. Sections were washed in malate buffer (100 mM maleic acid, 150 mM NaCl) and then in AP buffer (100 mM NaCl, 100 mM Tris-HCl, pH 9.5, 50 mM $MgCl_2$, 1% Tween-20). Tissue sections were treated with NBT/BCIP (Roche) mixture at room temperature in the dark for color development.

Fluorescence *in situ* hybridization (FISH) was performed as previously (Jiang *et al.* 2004). The PCR product from mouse *Homer1a* (NM_011982, sequence 1-167 bp) was inserted into the pSPT 18 vector (Roche). Probes were prepared from linearized plasmids using an SP6 or T7 RNA polymerase *in vitro* transcription kit (Roche). Slices were incubated with an AP-conjugated anti-DIG antibody at 4°C overnight. Signals were visualized by an incubation with an Alexa546 anti-sheep IgG antibody (Invitrogen, Carlsbad, CA, USA, RRID:AB_1500708) at room temperature for 2 h. Regarding the combination of FISH and immunohistochemistry, hybridized sections were incubated with an AP-conjugated anti-DIG and anti-Npas4 antibody (provided by Dr. Greenberg, RRID:AB_2687869) at 4°C overnight. Signals were visualized by an incubation with Alexa546 anti-sheep IgG and Alexa488 anti-rabbit IgG (Invitrogen, RRID:AB_141708) at room temperature for 2 h. Images were acquired with a Tie-A1 confocal microscope (Nikon, Sendai, Japan).

**Immunohistochemistry**

Mice were injected with tribromoethanol (200 mg/kg, i.p.) to lead rapid and deep anesthesia, and transcardially perfused with isotonic 0.1 M phosphate buffer (pH 7.4) followed by isotonic 4% PFA. The brain was post-fixed in 4% PFA at 4°C overnight, and then cryoprotected in 20-30% sucrose in 0.1 M phosphate buffer. Briefly, sections (20 μm) were fixed with 4% PFA and washed with 0.3% Triton X-100/PBS. They were incubated for 1 h in blocking serum (5% normal donkey serum in 0.2% Triton-X 100/PBS) and at 4°C for 24 h in the presence of the primary antibody (anti-Npas4; anti-Homer1a, Santa Cruz, Dallas, TX, USA, RRID:AB_675651; anti-neuronal nuclei (NeuN), sigma, RRID:AB_10711153;

anti-glial fibrillary acidic protein (GFAP), Sigma, RRID:AB_477010; anti-GFP, MBL, Nagoya, Japan, RRID:AB_591816). Sections were washed with PBS, and incubated with species-matched secondary antibodies (Alexa 488-conjugated anti-rabbit IgG; Alexa 488-conjugated anti-goat IgG, Invitrogen, RRID:AB_2534102; Alexa 546-conjugated anti-mouse IgG, Invitrogen, RRID:AB_2534012; Alexa 546-conjugated anti-goat IgG, Invitrogen, RRID:AB_142628) at room temperature for 1 h. Sections were imaged on the A1 confocal microscope (Nikon). The entire image of a coronal brain section was observed with a fluorescence microscope (BZ-9000, Keyence, Osaka, Japan).

**Immunoblotting**

Regarding the extraction of whole hippocampal lysates, tissues were homogenized in lysis buffer (20 mM Tris-HCl, pH 7.6, 150 mM NaCl, 1% NP-40, 0.1% SDS, 1% sodium deoxycholate, 2 mM EDTA, complete protease inhibitor cocktail (Roche), and phosSTOP phosphatase inhibitors (Roche)) at 20,000 × g at 4°C for 20 min. In order to extract plasma membrane proteins, hippocampal tissues were homogenized and extracted using the Membrane Protein Extraction Kit (BioVision, Milpitas, CA, USA). Protein lysates (10 μg) were subjected to SDS-PAGE and transferred to a polyvinylidene fluoride membrane (Immobilon-FL, Millipore, Bedford, MA, USA). Membranes were blocked with Blocking One P (Nacalai Tesque, Kyoto, Japan) or 1% skimmed milk in TBS-T (40 mM Tris, 0.3 M NaCl, and 0.1% Tween 20). The membrane was incubated with the primary antibody at 4°C overnight (Anti-Npas4; Anti-cFos, Santa Cruz, RRID:AB_2106765; Anti-β-Actin, Santa Cruz, RRID:AB_630835; Anti-Homer1a; Anti-Homer1c, Santa Cruz, RRID:AB_2121001;

Anti-GluA1, Millipore, RRID:AB_10680890; Anti-α1$Na^+/K^+$ ATPase, Abcam, Cambridge, MA, USA, RRID:AB_306023; Anti-N-Cadherin, Abcam, RRID:AB_444317), and incubated with HRP–conjugated secondary antibodies at room temperature for 1 h (HRP-conjugated anti-goat IgG, R&D Systems, Minneapolis, MN, USA, RRID:AB_357236; HRP-conjugated anti-rabbit IgG, GE Healthcare, Pittsburg, PA, USA, RRID:AB_772191). Bands were visualized using ECL Plus Western blotting detection reagents (GE Healthcare) and an imaging system (Atto Instruments, Tokyo, Japan). Band intensities were quantified using CS Analyzer Software (Atto Instruments).

**Luciferase assay**

The pGL4.10 [luc2] vector (Promega, Madison, WI, USA) was used in the present study. To create a pGL4.10-Homer1a promoter construct containing the mouse Homer1a promoter upstream of the luciferase gene, the Homer1a promoter was amplified by PCR from mouse genomic DNA. The following primers were used to prepare the Homer1a promoter construct: forward for -761/Luc, which includes a KpnI restriction site at the 5' end, 5'-GCCGGTACCGCGTGACATCATCCCCCGCACAAGCT-3'; reverse for -761/Luc, which includes KpnI restriction sites at the 5' end, 5'-GCCGGTACCCCCACCCCGGCTCGTCTCTCCCGCTC-3'. PCR products were digested with KpnI enzymes and then ligated into a pGL4.10 [luc2] vector that was digested with the same enzymes. PCR was used to create mutant #1/Luc, mutant #2/Luc, mutant #3/Luc, mutant #4/Luc, and mutant #1-4/Luc plasmids in which the putative Npas4 response element sequences of the Homer1a promoter were mutated. The primers used were as follows:

forward for mutant #1/Luc, 5'-CCGGCCGAGGGACATCATCCCCCGCACAA-3'; reverse for mutant #1/Luc, 5'-TGATGTCCCTCGGCCGGAAGTACTGCTAA-3'; forward for mutant #2/Luc, 5'-AAGCTGGAGGGAGCGGAGGGTGACGTATG-3'; reverse for mutant #2/Luc, 5'-TTCCGCTCCCTCCAGCTTGTGCGGGGGATG-3'; forward for mutant #3/Luc, 5'-CACCCGGAGGGCGGAGCGGACGAGGCCGT-3'; reverse for mutant #3/Luc, 5'-GCTCCGCCCTCCGGGTGCTCGCGCTGTGT-3'; forward for mutant #4/Luc, 5'-ACGAGGGAGGGGCGGCCCAGAGCCAGCGC-3'; reverse for mutant #4/Luc, 5'-GGCCGCCCCTCCCTCGTCCGCTCCGCACG -3'.

The luciferase assay was performed as described previously (Furukawa-Hibi *et al.* 2012). COS7 cells were plated on 24-well plates at 10,000 cells/well in Dulbecco's Modified Eagle's Medium (DMEM, Sigma-Aldrich) supplemented with 10% fetal bovine serum (Thermo Fisher Scientific) and antibiotics/antimycotics (Thermo Fisher Scientific) at 37°C in a humidified atmosphere with 5% $CO_2$. The next day, cells were transfected with 200 ng/well of the Npas4 plasmid or empty vector, 200 ng/well of the pGL4.10 or constructed Homer1a promoter/luc, and 30 ng/well of the phRG–TK construct, which expresses renilla luciferase, using Lipofectamine 2000 (Thermo Fisher Scientific) according to the manufacturer's protocol. The renilla luciferase construct was used as a control for transfection efficiency. After 24-36 h, cell lysates were prepared and assayed for luciferase activity using the Dual-Luciferase Reporter Assay System (Promega). Activity tests were performed and luminescence measured using a MiniLumat luminometer (Berthold, Wildbad, Germany).

**Hippocampal slice preparation and electrophysiology**

Hippocampal slices were prepared from the mice aged 8-12 weeks as described previously (Nakai *et al.* 2014). Mice were given an intraperitoneal injection of PTZ (45 mg/kg) 24 h prior to electrophysiological recordings and were decapitated under deep anesthesia with a combination anesthetic agent (i.p.) containing 0.15 mg/kg medetomidine, 2 mg/kg midazolam, and 2.5 mg/kg butorphanol. Brains were quickly removed, and 300-μm-thick slices were cut horizontally from the hippocampus using a vibratome in ice-cold modified artificial cerebrospinal fluid (ACSF) containing 206 mM sucrose, 5 mM KCl, 8 mM $MgCl_2$, 1.25 mM $KH_2PO_4$, 1 mM $CaCl_2$, 26 mM $NaHCO_3$, and 10 mM D-glucose. ACSF was gassed with 95% $O_2$ /5% $CO_2$ and pH was adjusted to 7.4. Slices were maintained at room temperature (26–28°C) for at least 1 h in an incubation chamber containing gassed standard ACSF containing 128 mM NaCl, 5 mM KCl, 1.3 mM $MgSO_4$, 1.25 mM $KH_2PO_4$, 2.41 mM $CaCl_2$, 26 mM $NaHCO_3$, and 10 mM D-glucose.

A single hippocampal slice was transferred to the recording chamber in which it was superfused continuously with gassed standard ACSF at a rate of 2–2.5 ml/min at 28–30°C. A stimulating electrode (monopolar stimulation) was positioned between the hilus and the CA3 cell layer and pushed 10–40 μm into the stratum lucidum to activate the mossy fiber (MF) (Jonas *et al.* 1993), or at the stratum radiatum of the CA3 region to activate associational/commissural fibers (AC). Constant-current pulses (50 μs) were supplied by a stimulator (SEN-3301, Nihon Kohden, Tokyo, Japan) every 20 s. The intensities of test stimuli were adjusted to evoke approximately 30–50% of the maximum response. In extracellular recordings, a glass pipette filled with 2 M NaCl (2–3 MΩ) was positioned at the stratum lucidum to record field excitatory postsynaptic potentials (fEPSPs) from MF-CA3 synapses or the stratum radiatum to record fEPSPs from AC-CA3 synapses. The stability of

the baseline was established by delivering test stimuli for 20-30 min before recordings. Responses from MF-CA3 synapses were identified if the group II metabotropic glutamate receptor agonist DCG-IV (1 μM) caused a more than 80% reduction in synaptic responses. The presynaptic fiber volley (PSFV) was recorded in the presence of the AMPAR blocker NBQX (10 μM) at the end of the experiments.

In whole-cell patch clamp recordings from CA3 pyramidal neurons in hippocampal slices, a patch electrode was filled with a pipette solution containing 140 mM K gluconate, 10 mM KCl, 2 mM $MgCl_2$, 0.2 mM EGTA, 10 mM HEPES, 3 mM Mg-ATP, and 0.3 mM Na-GTP (pH 7.2), with 6-8 MΩ of resistance. CA3 pyramidal neurons were imaged with IR-DIC optics (BX51WI with 20× water immersion objective lens, OLYMPUS, Tokyo, Japan). Holding potentials were compensated for by the junction potential between the pipette solution and external solution. AMPAR-mediated miniature excitatory postsynaptic currents (mEPSCs) were recorded in the voltage-clamp mode at a membrane potential of -70 mV, and in the presence of TTX (0.5 μM) and $GABA_A$ receptor antagonist picrotoxin (50 μM). Access resistance was monitored continuously during the experiment, and data obtained were discarded if access resistance fluctuated by more than 20%. Signals were amplified and filtered at 5 kHz with an amplifier (Axopatch 200B, Axon Instruments, Sunnyvale, CA, USA). Data acquisition and analyses were performed using pCLAMP 9.0 software (Axon Instruments).

**Adeno-associated virus (AAV) preparation and injection**

In order to construct an AAV vector, mouse Homer1a and Homer1c cDNA sequences were cloned into the multi cloning site (MCS) of the pAAV-CAGGS-EGFP-P2A-MCS plasmid as previously described (Nagai *et al.* 2016). AAV vectors were prepared and tittered as described previously (Sooksawate *et al.* 2013). Briefly, plasmids for the AAV vector, pHelper (Cell BioLabs, San Diego, CA, USA), and pAAV-DJ (Cell BioLabs) were transfected into HEK293 cells. After a 3-d incubation, cells were collected and purified. The titers of AAV were estimated by qPCR. Mice were anesthetized with tribromoethanol (250 mg/kg, i.p.) and positioned in a stereotaxic frame (David Kopf, Tujunga, CA, USA). The AAV virus (0.5 µl, $1.0\times10^{11}$ genome copies/ml) was injected into the hippocampus through a glass microinjection capillary tube at a rate of 0.1 µl/min (0.5 µl/site, six sites). The anteroposterior, mediolateral, and dorsoventral coordinates relative to the bregma were as follows (in mm): -2.0, ±1.8, -2.2; -2.0, ±1.8, -1.7; -2.8, ±3.0, -3.0.

**Statistical Analysis**

Researchers were blinded to the group allocation in all analyses. We could not reliably assess assumptions of how well normality and equal variances fit the data because the sample sizes were small. Sample size was not predetermined by formal power analysis statistical methods. No samples or data were excluded from the analysis. The sample number for each experiment is stated in the figures. Data analysis was performed using CS Analyzer Software (Atto Instruments), pCLAMP 9.0 software (Axon Instruments), and IBM SPSS Statistics 24 (IBM, Tokyo, Japan). All data are expressed as means ± SEM. A one-way, two-way, or three-way analysis of variance (ANOVA) was used, followed by Tukey's test when the F

ratios were significant ($p<0.05$). Significant differences between two groups were assessed using the Student's T-test.

## Results

### Homeostatic control of kindling epileptogenesis by Npas4

Repeated treatments with a sub-convulsive dosage of PTZ, a $GABA_A$ receptor antagonist, is known to induce kindling, which is a commonly preferred animal model used to study epilepsy (Morimoto *et al.* 2004, Dhir 2012). C57BL/6 mice were intraperitoneally (i.p.) administered different dosages of PTZ to induce convulsive seizures. We monitored mouse behaviors for 20 min after the PTZ injection, and scored the seizure level of mice (Fig. S1a). Although a low dose of PTZ (25 mg/kg) had a negligible effect on the seizure score, a high dose of PTZ (45 mg/kg) induced a seizure characterized by tonic convulsions, jumping, and/or running (Fig. S1b). Therefore, C57BL/6 mice were repeatedly administered the sub-convulsive dose of PTZ (25 mg/kg) every 48 h to achieve the fully kindled state (Fig. 1a). A total of 16 injections of PTZ were required for the development of kindling, whereas no marked change in the seizure score was observed with repeated saline injections and a repeated saline plus single treatment with PTZ at the last injection (injections, $F(15,270)=12.71$, $p<0.01$; PTZ treatment, $F(2,18)=149.70$, $p<0.01$; interaction, $F(30,270)=10.13$, $p<0.01$; two-way ANOVA; Fig. 1b).

We assessed *cFos* mRNA expression, as a measure of neuronal excitation, in the hippocampus of mice 1 h after the last treatment with PTZ (Fig. 1c). *cFos* mRNA levels were higher in repeated PTZ-treated kindled mice than in saline-treated control or single

PTZ-treated mice ($F(2,7)=38.6$, $p<0.01$; one-way ANOVA; Fig. 1d). The expression level of *Npas4* mRNA was also significantly higher after the repeated PTZ treatment than in saline-treated or single PTZ-treated mice ($F(2,7)=38.6$, $p<0.01$; one-way ANOVA; Fig. 1d). A single treatment with PTZ had no effect on *Npas4* mRNA levels (Fig. 1d). These results indicate that Npas4, as well as cFos, is induced in the hippocampus of kindled mice in an activity-dependent manner.

In order to investigate whether Npas4 participates in the sensitivity of convulsions and/or epileptogenesis, wild-type and *Npas4* knockout (*Npas4* KO) mice were monitored for PTZ-induced convulsive seizures and kindling. PTZ-induced convulsive seizures were observed in wild-type and *Npase4* KO mice, and the scores of *Npas4* KO mice were similar to those of wild-type mice (Fig. S1). When the time course for the development of PTZ-induced kindling was compared between wild-type and *Npas4* KO mice, *Npas4* KO mice developed kindling more rapidly than their wild-type littermates (injection, $F(8,96)=18.12$, $p<0.01$; genotype, $F(1,12)=36.00$, $p<0.01$; PTZ treatment, $F(1,12)=286.29$, $p<0.01$; genotype×PTZ treatment interaction, $F(1,12)=30.35$, $p<0.01$; genotype×injection interaction, $F(8,96)=3.19$, $p<0.01$; PTZ treatment×injection interaction, $F(8,96)=12.50$, $p<0.01$; genotype×PTZ treatment×injection interaction, $F(8,96)=0.94$, $p=0.49$; three-way ANOVA with repeated measures; Fig. 1e). Consistent with behavioral observations, the expression level of *cFos* mRNA in the hippocampus of repeated PTZ-treated *Npas4* KO mice was significantly higher than that in wild-type mice after 9 PTZ injections (genotype, $F(1,12)=34.38$, $p<0.01$; PTZ treatment, $F(1,12)=140.6$, $p<0.01$; interaction, $F(1,12)=0.01$, $p=0.93$; two-way ANOVA; Fig. 1f), which was similar to the level detected in fully kindled wild-type animals (Fig. 1d). These results suggest that Npas4 serves as a homeostatic factor in epileptogenesis.

**Spatiotemporal expression of Npas4 after convulsive seizures**

In order to clarify the mechanisms by which Npas4 regulates the development of kindling, we investigated the temporal dynamics of Npas4 and cFos expression in the hippocampus of wild-type mice after convulsive seizures induced by a single injection of PTZ (45 mg/kg, Fig. 2a). The expression of *Npas4* and *cFos* mRNA was significantly increased in the hippocampus 0.5 and 1 h after the PTZ treatment, and returned to the basal level within 2 h (*Npas4* mRNA, $F(6,21)=21.97$, $p<0.01$; *cFos* mRNA $F(6, 21)=86.72$, $p<0.01$; one-way ANOVA; Fig. 2b and S2). *Npas4* mRNA expression was the most prominent in the entire hippocampal CA subregions and dentate gyrus 1 h after the PTZ treatment (Fig. 2c); these areas are often associated with epileptic activity in humans and animal models of limbic epilepsy (Cavus *et al.* 2008, Gelinas *et al.* 2016). *Npas4* mRNA was virtually undetectable in the hippocampus of *Npas4* KO mice after the saline or PTZ injection (Fig. 2c). Immunoblotting analyses revealed that Npas4 and cFos protein levels were increased in the hippocampus 2 h after the PTZ treatment, and then returned to basal levels within 4 h (Npas4, $F(5,18)=10.59$, $p<0.01$; cFos, $F(5,18)=50.31$, $p<0.01$; one-way ANOVA; Fig. 2d). The Npas4 protein was detected in the CA subregions and dentate gyrus after the PTZ treatment (Fig. 2e).

**PTZ-induced convulsive seizures promote Homer1a expression in the hippocampus**

We examined Npas4 target genes that may serve as homeostatic factors in the epileptogenesis of PTZ-induced kindling. Based on previous chromatin immunoprecipitation (ChIP) sequencing screens and microarray studies on Npas4 target genes (Lin *et al.* 2008,

Yoshihara *et al.* 2014), we focused on Homer1a. Homer1a is induced by an epileptic stimulus (Cavarsan *et al.* 2012) and mediates the homeostatic scaling-down of excitatory synapses (Diering *et al.* 2017, Hu *et al.* 2010). In order to establish whether convulsive seizures affect Homer1a expression, we characterized *Homer1a* mRNA expression in response to the PTZ treatment (45 mg/kg, Fig. 3a). The expression of *Homer1a* mRNA in the hippocampus increased 2 h and 4 h after seizure activity, and returned to basal levels within 8 h ($F(5,18)=120.2$, $p<0.01$; one-way ANOVA; Fig. 3b). The expression of *Homer1a* mRNA after the PTZ treatment was the most prominent in the hippocampal CA sub-regions and dentate gyrus (Fig. 3c). Homer1a protein levels also increased in the hippocampus, and peaked 4 h after the PTZ treatment ($F(5,18)=26.44$, $p<0.01$; one-way ANOVA; Fig. 3d). However, the expression of Homer1c, a constitutive and longer isoform of Homer1, was constant, even after the PTZ treatment (Fig. S3). Double-labeling immunohistochemistry revealed that Homer1a-positive cells co-localized with NeuN-positive neurons, but not GFAP-positive astrocytes, in the CA3 sub-region of the hippocampus after the PTZ treatment (Fig. 3e), indicating that the seizure-induced up-regulation of Homer1a predominantly occurs in neurons in the hippocampus.

**Npas4 mediates PTZ-induced Homer1a expression in the hippocampus**

A previous study demonstrated that Npas4 binds to a critical CGTG core element in the promoter of its target genes (Ooe *et al.* 2004). Since we identified 4 potential regulatory elements of Npas4 in the *Homer1a* promoter region, the corresponding genomic fragments (761 bp) of the promoter region were cloned into a luciferase reporter plasmid. COS7 cells were co-transfected with luciferase reporter plasmids including the *Homer1a* promoter with

or without the *Npas4* plasmid. Promoter activity was measured 24-36 h after transfection (Fig. 4a). Compared with control cells, Npas4 co-transfected cells showed increased relative luciferase activity of more than 400% of the corresponding control cells (Homer1a promoter, $F(1,42)=91.8$, $p<0.01$; Npas4, $F(1,42)=43.84$, $p<0.01$; interaction, $F(1,42)=43.23$, $p<0.01$; two-way ANOVA; Fig. 4b).

We subsequently attempted to identify certain functional elements in the promoter that may be activated by Npas4. Any one of 4 putative Npas4 response elements or all of them in the Homer1a promoter were replaced by GAGGG sequences (Fig. 4c). The mutation of Npas4 response element #3, #4, or #1-4 significantly decreased Homer1a promoter activity, whereas the other two mutants (#1 and #2 mutant) had negligible effects ($F(5,65)=52.77$, $p<0.01$; one-way ANOVA; Fig. 4c). These results suggest that the proximal region around the core promoter of Homer1a contains 2 positive regulatory Npas4 response elements that contribute to the induction of Homer1a.

The present results strongly suggest that Homer1a acts as a downstream target gene in Npas4 signaling in response to convulsive seizures and kindling. In order to obtain further evidence in support of this hypothesis and confirm the cellular mechanisms underlying this effect, we employed *Npas4* KO mice treated with PTZ (Fig. 4d). The PTZ-stimulated induction of Homer1a mRNA and protein was attenuated in the hippocampus of *Npas4* KO mice (*Homer1a* mRNA; genotype, $F(1,12)=11.70$, $p<0.01$; PTZ treatment, $F(1,12)=73.69$, $p<0.01$; interaction, $F(1,12)=11.12$, $p<0.01$; Homer1a protein; genotype, $F(1,8)=38.82$, $p<0.01$; PTZ treatment, $F(1,8)=73.73$, $p<0.01$; interaction, $F(1,8)=34.97$, $p<0.01$; two-way ANOVA; Fig. 4e and 4f). The combination of FISH and immunohistochemical analyses revealed that *Homer1a* mRNA co-localized with the Npas4 protein 2 h after the convulsive

seizure response (Fig. 4g). The PTZ treatment increased cFos mRNA and protein expression in the hippocampus of *Npas4* KO mice as well as wild-type mice (Fig. S4a and S4b). Homer1c mRNA and protein levels in the hippocampus were similar between *Npas4 KO* and wild-type mice with or without the PTZ treatment (Fig. S4c and S4d). These results indicate that Npas4 promotes Homer1a expression in the hippocampus after convulsive seizures without affecting neuronal responses to PTZ or the constitutive expression of a longer form of Homer1c.

**Npas4 adapts homeostatic scaling though surface AMPAR expression after convulsive seizure responses**

Synaptic scaling, a form of neural plasticity, maintains the fundamental properties of neuronal homeostasis after hyper- or hypo-excitation of the network (Turrigiano 2008, Ibata *et al.* 2008). We analyzed AMPAR GluA1 subunit levels in the plasma membrane fraction extracted from the hippocampus of PTZ-treated mice (Fig. 5a). Surface AMPAR GluA1 subunit levels significantly decreased 24 h after the PTZ treatment and this reduction was maintained at least up to 48 h later ($F(3,12)=16.77$, $p<0.01$; one-way ANOVA; Fig. 5b). The PTZ treatment had no effect on total AMPAR GluA1 subunit levels (Fig. S5a). We then investigated whether Npas4 is involved in the down-regulation of surface AMPAR GluA1 expression after seizure activity. *Npas4* KO mice were treated with PTZ, and the surface membrane protein was extracted from the hippocampus 24 h after the treatment. Reductions in AMPAR GluA1 subunit levels in the membrane fraction after the PTZ treatment were attenuated in *Npas4* KO mice (genotype, $F(1,20)=30.43$, $p<0.01$; PTZ treatment, $F(1,20)=75.82$, $p<0.01$; interaction, $F(1,20)=5.11$, $p<0.01$; two-way ANOVA; Fig. 5c), while

total AMPAR GluA1 levels were similar between *Npas4* KO and wild-type mice (Fig. S5b). Furthermore, a significant difference was observed in normalized surface GluA1 levels after the PTZ treatment between wild-type and *Npas4* KO mice. These results suggest that Npas4 controls the surface expression of AMPARs in the hippocampus after convulsive seizure responses.

**Npas4 reduces excitatory synaptic transmission in the hippocampus after convulsive seizure responses**

To clarify the physiological significance of reductions in the surface expression of AMPARs in the hippocampus after convulsive seizures, we examined the strength of evoked synaptic transmission at MF-CA3 synapses and AC-CA3 synapses in wild-type and *Npas4* KO mice with or without an injection of PTZ (45 mg/kg, Fig. 5a). PTZ significantly reduced the fEPSP/PSFV ratio at AC-CA3 synapses in wild-type mice, whereas it had no effect on that in *Npas4* KO mice (genotype, $F(1,29)=10.64$, $p<0.01$; PTZ treatment, $F(1,29)=6.16$, $p<0.01$; interaction, $F(1,29)=20.41$, $p<0.01$; two-way ANOVA; Fig. 5d). Furthermore, a significant difference was observed in the fEPSC/PSFV ratio after the PTZ treatment between wild-type and *Npas4* KO mice. On the other hand, the fEPSP/PSFV ratio at MF-CA3 synapses was not altered by PTZ in wild-type or *Npas4* KO mice (Fig. S5c), suggesting that convulsive seizure responses affect synaptic transmission evoked at AC-CA3 synapses rather than at MF-CA3 synapses.

To examine whether PTZ modulates the probability of glutamate release from MF and AC, we measured mEPSCs in hippocampal CA3 neurons from wild-type and *Npas4* KO mice. PTZ significantly reduced the average amplitude of mEPSCs in wild-type mice, but not in

*Npas4* KO mice (genotype, $F(1,19)=4.90$, $p<0.01$; PTZ treatment, $F(1,19)=1.66$, $p=0.21$; genotype×PTZ interaction, $F(1,19)=16.11$, $p<0.01$; two-way ANOVA; Fig. 5e). Furthermore, a significant difference in the average amplitude of mEPSCs was evident between wild-type and *Npas4* KO mice after the PTZ treatment. On the other hand, the frequency of their generation was slightly increased by PTZ in wild-type and *Npas4* KO mice (Fig S5d).

To predominantly observe synaptic inputs from AC-CA3 synapses, we measured mEPSCs in the presence of the group II metabotropic glutamate receptor agonist DCG-IV, which selectively suppresses synaptic transmission at MF-CA3 synapses, but not at AC-CA3 synapses (Kamiya *et al.* 1996). The frequency of mEPSCs was decreased by DCG-IV in all groups, presumably due to the inhibition of synaptic inputs from MF (Fig. S5d). However, the significant difference observed in the average amplitude of mEPSCs after the PTZ treatment between wild-type and *Npas4* KO mice was not affected by the presence or absence of DCG-IV (genotype, $F(1,38)=11.67$, $p<0.01$; PTZ treatment, $F(1,38)=8.17$, $p<0.01$; DCG-IV treatment, $F(1,38)=0.99$, $p=0.32$; genotype×PTZ interaction, $F(1,38)=39.30$, $p<0.01$; PTZ treatment×DCG-IV treatment interaction, $F(1,38)=1.03$, $p=0.32$; genotype×PTZ treatment×DCG-IV treatment interaction, $F(1,38)=0.28$, $p=0.60$; three-way ANOVA; Fig. 5e). Collectively, these results suggest that PTZ reduces excitatory synaptic transmission at AC-CA3 synapses through the Npas4-mediated down-regulation of postsynaptic AMPARs in hippocampal CA3 neurons.

**Npas4 controls homeostatic scaling during kindling development though Homer1a**

In order to investigate whether the expression of Homer1a in the hippocampus rescues the accelerated development of PTZ-induced kindling in *Npas4* KO mice, we bilaterally

microinjected AAV, which promotes the expression of Homer1a, into the hippocampus of *Npas4* KO mice (Fig. 6a and b). Immunohistochemistry revealed the exclusive expression of the Homer1a protein and no gross abnormalities in the hippocampus of AAV-Homer1a-microinjected mice (Fig. 6c). The AAV-mediated expression of Homer1a resulted in lower AMPAR GluA1 subunit levels in the hippocampal plasma membrane fraction than in that from AAV-EGFP-transfected *Npas4* KO mice ($F(2,9)=8.058$, $p<0.01$; one-way ANOVA; Fig. 6d), whereas it had no effect on total GluA1 subunit levels (Fig. S6). We also monitored kindling development induced by a sub-convulsive dose of PTZ (Fig. 6a). The development of kindling was more strongly suppressed in AAV-*Homer1a*-microinjeted *Npas4* KO mice than in AAV-*EGFP*-microinjected *Npas4* KO mice, whereas the seizure threshold was not affected after the first injection (AAV treatment, $F(2,10)=10.45$, $p<0.01$; PTZ treatment, $F(9,90)=71.22$, $p<0.01$; interaction, $F(18,90)=1.57$, $p<0.01$; two-way ANOVA; Fig. 6e). No significant difference was observed between AAV-*Homer1c* and AAV-*EGFP*-microinjected *Npas4* KO mice (Fig. 6d and 6e). These results indicate that Homer1a, but not Homer1c is required for Npas4-mediated homeostatic scaling during kindling development.

## Discussion

The main result of the present study is that Npas4 functions as an intrinsic modulator of seizure activity and epileptogenesis. This conclusion is supported by several results. We demonstrated that Npas4 is selectively up-regulated in the hippocampus in response to seizure activity induced by convulsive doses of PTZ or PTZ-induced kindling. A defect in the Npas4 gene facilitated the development of kindling. Furthermore, the loss of Npas4 impaired

homeostatic scaling in the hippocampus with the down-regulation of surface AMPARs expression. In addition, the expression of Homer1a in the hippocampus of *Npas4* KO mice rescued the disturbance in homeostatic scaling during kindling development. Collectively, the present results suggest that Npas4 controls neuronal homeostatic scaling during epileptogenesis through the induction of Homer1a as negative feedback machinery for the management of epilepsy.

Seizure activity evoked by diverse stimuli, such as structural damage, electrical stimuli, or chemical agents, triggers a signaling cascade that culminates in the expression of many genes including the immediate-early response gene *Npas4* (Renier *et al.* 2016). A previous study demonstrated that Npas4 signaling was up-regulated by neuronal excitability (Lin *et al.* 2008). We showed that Npas4 was up-regulated within 2 h of seizure activity in a single PTZ-induced convulsive seizure model and repeated PTZ-induced kindling model. Treatment with PTZ has been shown to increase the release of glutamate by blocking $GABA_A$ receptors (Feng *et al.* 2005). The expression of Npas4 is induced by $Ca^{2+}$ influx through voltage-gated channels, but not by increased cAMP concentrations or neurotrophic factors (Lin *et al.* 2008, Speckmann *et al.* 2016). Therefore, Npas4 may be immediately induced in response to excitatory glutamatergic inputs after seizure responses.

*Bdnf* is one of the major target genes for Npas4 (Lin *et al.* 2008). Cumulative evidence in recent years has highlighted the importance of BDNF and its signaling through the TrkB receptor in limbic epileptogenesis (Liu *et al.* 2013, Gu *et al.* 2015). Our previous findings also demonstrated that BDNF expression was increased in the hippocampus in response to PTZ-induced kindling (Mizoguchi *et al.* 2011). Epileptic conditions have been reported to increase the expression level of BDNF (Ernfors *et al.* 1991, Altar *et al.* 2004). Furthermore,

*Bdnf* heterozygous KO mice showed a marked reduction in the rate of kindling development (Kokaia *et al.* 1995), while the infusion of BDNF into the rat hippocampus induced seizures (Scharfman *et al.* 2002). Accordingly, we assumed that the development of PTZ-induced kindling occurred later or was weaker in *Npas4* KO mice than in wild-type mice. However, *Npas4* KO mice exhibited the accelerated development of PTZ-induced kindling, suggesting that Npas4 serves as a critical negative feedback factor to suppress the development of kindling. This negative feedback factor induced by Npas4 appears to have a greater impact on epileptogenesis than BDNF. These results are consistent with the brain's capacity for activity-dependent self-regulation, and suggest a novel intrinsic mechanism by which Npas4 adapts to and represses epileptic conditions (O'Leary and Wyllie 2011, Ibata *et al.* 2008).

It has been demonstrated that Npas4 interacts with Homer1a gene in the mouse brain using ChIP sequencing analysis (Yoshihara *et al.* 2014). The promoter region of *Homer1* contains several response elements for transcription factors including CRE-binding protein (CREB) and Npas4. PTZ has been shown to decrease the phosphorylation levels of CREB in the hippocampus of rats (Ullah *et al.* 2015). In the present study, we demonstrated that Npas4 increased *Homer1a* promoter activity in COS7 cells through Npas4 response elements. The PTZ treatment increased *Homer1a* mRNA and protein levels, and the induction of Homer1a was markedly attenuated in the hippocampus of *Npas4* KO mice. Furthermore, co-localization of the Npas4 protein and *Homer1a* mRNA was observed in the hippocampus of PTZ-treated mice. These results indicate that Homer1a is one of the Npas4 target genes.

Homer1 belongs to a family of scaffolding proteins that localize at the PSD (Hayashi *et al.* 2009). Homer1 proteins are primarily classified into two isoforms. The long form of Homer1 (Homer1L) including Homer1c is constitutively expressed and consists of an

N-terminal EVH1-binding domain followed by a coiled-coil domain that mediates dimerization with other Homer proteins. The EVH1-binding domain of Homer1 binds to Shank, group I metabotropic glutamate receptors (mGluR1/5), inositol-1,4,5-triphosphate (IP3) receptors, and ryanodine receptors (Shiraishi-Yamaguchi and Furuichi 2007). Homer1a is the short form of Homer1 and is induced in an activity-dependent manner. Homer1a has the ability to interact with PSD target proteins, but cannot self-assemble because it lacks the C-terminal coiled-coil domain. Therefore, Homer1a is regarded as a dominant negative regulator that interferes with PSD complexes (Shiraishi-Yamaguchi and Furuichi 2007).

Homeostatic adaptation is associated with alterations in postsynaptic AMPAR expression at excitatory synapses which is through removal and dephosphorylating of synaptic AMPARs and this process is mediated by alterations in the signaling of protein kinase A and mGluR1/5 (Cavarsan *et al.* 2012, Diering *et al.* 2017). It has been suggested to occur in a manner that maintains relative synaptic strength by effectively scaling all synapses (Turrigiano 2008). Many studies have provided strong evidence that AMPARs undergo rapid recycling in the postsynaptic compartment. Hu *et al.* (2010) demonstrated that Homer1a expression reduced the tyrosine phosphorylation of GluA2 through agonist-independent mGluR1/5 activity, and its tyrosine phosphorylation regulated GluA2 trafficking followed by a reduction of AMPAR-mediated synaptic strength, thereby playing an indispensable role in the expression of certain forms of synaptic plasticity. The expression of Homer1a has been shown to decrease the postsynaptic protein Shank in spines, and inhibit postsynaptic AMPAR and NMDAR currents in the hippocampal neurons (Sala *et al.* 2003), while the homeostatic scaling of AMPARs is impaired in the primary cultured cortical neurons of *Homer1a* KO mice (Hu *et al.* 2010). In the present study, PTZ treatment decreased the surface expression of

the AMPAR GluA1 subunit and AMPAR-mediated mEPSCs at AC-CA3 synapses in the hippocampus of wild-type mice 24 h after the treatment. The PTZ-induced down-regulation of AMPAR GluA1 was attenuated in *Npas4* KO mice. *Npas4* KO mice did not show the PTZ-induced reductions in AMPAR-mediated mEPSCs at AC-CA3 synapses. Collectively, these results suggest that neuronal hyperexcitability induced by PTZ treatment leads to a down-regulation of postsynaptic AMPARs in the hippocampal CA3 neurons of wild-type mice to induce compensatory changes in excitatory synaptic transmission within 24 h, whereas *Npas4* KO mice lacked the capability to down-regulate postsynaptic AMPARs after PTZ treatment.

The application of AAV-Homer1a to the hippocampus of *Npas4* KO mice promoted the down-regulation of surface AMPAR GluA1 subunit expression and normalized the facilitated development of kindling induced by PTZ. Transgenic mice that express Homer1a showed the attenuation of electrical stimulation-induced kindling (Potschka *et al.* 2002). The expression of Homer1a reduces synaptic AMPAR-mediated currents recorded from pyramidal neurons in organotypic cultures of hippocampal slices (Sala *et al.* 2003). Previous studies demonstrated that Homer1a regulated the homeostatic scaling of AMPARs through mGluR1/5 (Diering *et al.* 2017, Hu *et al.* 2010). Homer1a in PSD binds to mGluR1/5 and activates signaling to promote AMPAR endocytosis (Hu *et al.* 2010). Thus, homeostatic scaling by Npas4-Homer1a signaling may lead though affecting the function of the mGluR1/5-HomerL-IP3R complex.

In conclusion, our results highlighted a previously unknown mechanism of Npas4 that contributes to epileptogenesis and is dependent on Home1a transcription *in vivo*. The Npas4-dependent expression of Homer1a may be required for maintaining excitation of the

neuronal network through the adaptation of homeostatic scaling by AMPAR endocytosis after seizure activity. Based on the results of the present study, we propose that Npas4 functions as a molecular switch to initiate homeostatic scaling and the targeting of Npas4-Homer1a signaling may provide new approaches for the treatment of epilepsy.

**Acknowledgments**

We thank Dr. Michael E. Greenberg for providing *Npas4* KO mice. We also thank Division for Research on Laboratory Animals and Medical Research Engineering of Nagoya University Graduate School of Medicine. This work was supported by the following funding sources: KAKENHI Grant Numbers JP17H04031, JP17H02220, JP16K15201, JP15H01284, and 25116515 from JSPS, the SRPBS from AMED, Research on Regulatory Science of Pharmaceuticals and Medical Devices from AMED, a Grant for Biomedical Research from SRF, the Astellas Foundation for Research on Metabolic Disorders.

## References


Altar C. A., Laeng P., Jurata L. W. et al. (2004) Electroconvulsive seizures regulate gene expression of distinct neurotrophic signaling pathways. *J. Neurosci.* **24,** 2667-2677.

Bell G. S., Neligan A. and Sander J. W. (2014) An unknown quantity-the worldwide prevalence of epilepsy. *Epilepsia* **55,** 958-962.

Cavarsan C. F., Tescarollo F., Tesone-Coelho C., Morais R. L., Motta F. L., Blanco M. M. and Mello L. E. (2012) Pilocarpine-induced status epilepticus increases Homer1a and changes mGluR5 expression. *Epilepsy Res.* **101,** 253-260.

Cavus I., Pan J. W., Hetherington H. P., Abi-Saab W., Zaveri H. P., Vives K. P., Krystal J. H., Spencer S. S. and Spencer D. D. (2008) Decreased hippocampal volume on MRI is associated with increased extracellular glutamate in epilepsy patients. *Epilepsia* **49,** 1358-1366.

Dhir A. (2012) Pentylenetetrazol (PTZ) kindling model of epilepsy. *Curr. Protoc. Neurosci.* **Chapter 9,** Unit9.37.

Diering G. H., Nirujogi R. S., Roth R. H., Worley P. F., Pandey A. and Huganir R. L. (2017) Homer1a drives homeostatic scaling-down of excitatory synapses during sleep. *Science* **355,** 511-515.

Erdtmann-Vourliotis M., Riechert U., Mayer P., Grecksch G. and Hollt V. (1998) Pentylenetetrazole (PTZ)-induced c-fos expression in the hippocampus of kindled rats is suppressed by concomitant treatment with naloxone. *Brain Res.* **792,** 299-308.

Ernfors P., Bengzon J., Kokaia Z., Persson H. and Lindvall O. (1991) Increased levels of messenger RNAs for neurotrophic factors in the brain during kindling epileptogenesis. *Neuron* **7,** 165-176.

Feng S., Ma S., Jia C. et al. (2016) Sonic hedgehog is a regulator of extracellular glutamate levels and epilepsy. *EMBO Rep.* **17,** 682-694.

Feng Y., LeBlanc M. H. and Regunathan S. (2005) Agmatine reduces extracellular glutamate during pentylenetetrazole-induced seizures in rat brain: a potential mechanism for the anticonvulsive effects. *Neurosci. Lett.* **390,** 129-133.

Ferraro T. N., Golden G. T., Smith G. G. et al. (1999) Mapping loci for pentylenetetrazol-induced seizure susceptibility in mice. *J. Neurosci.* **19,** 6733-6739.

Furukawa-Hibi Y., Yun J., Nagai T. and Yamada K. (2012) Transcriptional suppression of the neuronal PAS domain 4 (Npas4) gene by stress via the binding of agonist-bound glucocorticoid receptor to its promoter. *J. Neurochem.* **123,** 866-875.

Galanopoulou A. S., Buckmaster P. S., Staley K. J. et al. (2012) Identification of new epilepsy treatments: issues in preclinical methodology. *Epilepsia* **53,** 571-582.

Gelinas J. N., Khodagholy D., Thesen T., Devinsky O. and Buzsaki G. (2016) Interictal epileptiform discharges induce hippocampal-cortical coupling in temporal lobe epilepsy. *Nat. Med.* **22,** 641-648.

Gu B., Huang Y. Z., He X. P., Joshi R. B., Jang W. and McNamara J. O. (2015) A Peptide Uncoupling BDNF Receptor TrkB from Phospholipase Cgamma1 Prevents Epilepsy Induced by Status Epilepticus. *Neuron* **88,** 484-491.

Hayashi M. K., Tang C., Verpelli C., Narayanan R., Stearns M. H., Xu R. M., Li H., Sala C. and Hayashi Y. (2009) The postsynaptic density proteins Homer and Shank form a polymeric network structure. *Cell* **137,** 159-171.

Hu J. H., Park J. M., Park S. et al. (2010) Homeostatic scaling requires group I mGluR activation mediated by Homer1a. *Neuron* **68,** 1128-1142.

Ibata K., Sun Q. and Turrigiano G. G. (2008) Rapid synaptic scaling induced by changes in postsynaptic firing. *Neuron* **57,** 819-826.

Jiang H., Mankodi A., Swanson M. S., Moxley R. T. and Thornton C. A. (2004) Myotonic dystrophy type 1 is associated with nuclear foci of mutant RNA, sequestration of muscleblind proteins and deregulated alternative splicing in neurons. *Hum. Mol. Genet.* **13,** 3079-3088.

Jonas P., Major G. and Sakmann B. (1993) Quantal components of unitary EPSCs at the mossy fibre synapse on CA3 pyramidal cells of rat hippocampus. *J. Physiol.* **472,** 615-663.

Kamiya H., Shinozaki H. and Yamamoto C. (1996) Activation of metabotropic glutamate receptor type 2/3 suppresses transmission at rat hippocampal mossy fibre synapses. *J. Physiol.* **493 ( Pt 2),** 447-455.

Kokaia M., Ernfors P., Kokaia Z., Elmer E., Jaenisch R. and Lindvall O. (1995) Suppressed epileptogenesis in BDNF mutant mice. *Exp. Neurol.* **133,** 215-224.

Kwan P., Schachter S. C. and Brodie M. J. (2011) Drug-resistant epilepsy. *N. Engl. J. Med.* **365,** 919-926.

Li K. X., Lu Y. M., Xu Z. H. et al. (2011) Neuregulin 1 regulates excitability of fast-spiking neurons through Kv1.1 and acts in epilepsy. *Nat. Neurosci.* **15,** 267-273.

Lin Y., Bloodgood B. L., Hauser J. L., Lapan A. D., Koon A. C., Kim T. K., Hu L. S., Malik A. N. and Greenberg M. E. (2008) Activity-dependent regulation of inhibitory synapse development by Npas4. *Nature* **455,** 1198-1204.

Liu G., Gu B., He X. P., Joshi R. B., Wackerle H. D., Rodriguiz R. M., Wetsel W. C. and McNamara J. O. (2013) Transient inhibition of TrkB kinase after status epilepticus prevents development of temporal lobe epilepsy. *Neuron* **79,** 31-38.

Loscher W., Klitgaard H., Twyman R. E. and Schmidt D. (2013) New avenues for anti-epileptic drug discovery and development. *Nat. Rev. Drug Discov.* **12,** 757-776.

Mizoguchi H., Nakade J., Tachibana M. et al. (2011) Matrix metalloproteinase-9 contributes to kindled seizure development in pentylenetetrazole-treated mice by converting pro-BDNF to mature BDNF in the hippocampus. *J. Neurosci.* **31,** 12963-12971.

Morimoto K., Fahnestock M. and Racine R. J. (2004) Kindling and status epilepticus models of epilepsy: rewiring the brain. *Prog. Neurobiol.* **73,** 1-60.

Nagai T., Nakamuta S., Kuroda K. et al. (2016) Phosphoproteomics of the dopamine pathway enables discovery of Rap1 activation as a reward signal *In vivo*. *Neuron* **89,** 550-565.

Nakai T., Nagai T., Tanaka M. et al. (2014) Girdin phosphorylation is crucial for synaptic plasticity and memory: a potential role in the interaction of BDNF/TrkB/Akt signaling with NMDA receptor. *J. Neurosci.* **34,** 14995-15008.

O'Leary T. and Wyllie D. J. (2011) Neuronal homeostasis: time for a change? *J. Physiol.* **589,** 4811-4826.

Ooe N., Saito K., Mikami N., Nakatuka I. and Kaneko H. (2004) Identification of a novel basic helix-loop-helix-PAS factor, NXF, reveals a Sim2 competitive, positive regulatory role in dendritic-cytoskeleton modulator drebrin gene expression. *Mol. Cell. Biol.* **24,** 608-616.

Potschka H., Krupp E., Ebert U. et al. (2002) Kindling-induced overexpression of Homer 1A and its functional implications for epileptogenesis. *Eur. J. Neurosci.* **16,** 2157-2165.

Ramamoorthi K., Fropf R., Belfort G. M., Fitzmaurice H. L., McKinney R. M., Neve R. L., Otto T. and Lin Y. (2011) Npas4 regulates a transcriptional program in CA3 required for contextual memory formation. *Science* **334,** 1669-1675.

Renier N., Adams E. L., Kirst C. et al. (2016) Mapping of brain activity by automated volume analysis of immediate early genes. *Cell* **165,** 1789-1802.

Sala C., Futai K., Yamamoto K., Worley P. F., Hayashi Y. and Sheng M. (2003) Inhibition of dendritic spine morphogenesis and synaptic transmission by activity-inducible protein Homer1a. *J. Neurosci.* **23,** 6327-6337.

Scharfman H. E., Goodman J. H., Sollas A. L. and Croll S. D. (2002) Spontaneous limbic seizures after intrahippocampal infusion of brain-derived neurotrophic factor. *Exp. Neurol.* **174,** 201-214.

Seeburg D. P. and Sheng M. (2008) Activity-induced Polo-like kinase 2 is required for homeostatic plasticity of hippocampal neurons during epileptiform activity. *J Neurosci* **28,** 6583-6591.

Shiraishi-Yamaguchi Y. and Furuichi T. (2007) The Homer family proteins. *Genome Biol.* **8,** 206.

Sim S., Antolin S., Lin C. W., Lin Y. and Lois C. (2013) Increased cell-intrinsic excitability induces synaptic changes in new neurons in the adult dentate gyrus that require Npas4. *J. Neurosci.* **33,** 7928-7940.

Sooksawate T., Isa K., Matsui R., Kato S., Kinoshita M., Kobayashi K., Watanabe D., Kobayashi K. and Isa T. (2013) Viral vector-mediated selective and reversible blockade of the pathway for visual orienting in mice. *Front. Neural Circuits* **7,** 162.

Speckmann T., Sabatini P. V., Nian C., Smith R. G. and Lynn F. C. (2016) Npas4 Transcription Factor Expression Is Regulated by Calcium Signaling Pathways and Prevents Tacrolimus-induced Cytotoxicity in Pancreatic Beta Cells. *J. Biol. Chem.* **291,** 2682-2695.

Spiegel I., Mardinly A. R., Gabel H. W., Bazinet J. E., Couch C. H., Tzeng C. P., Harmin D. A. and Greenberg M. E. (2014) Npas4 regulates excitatory-inhibitory balance within neural circuits through cell-type-specific gene programs. *Cell* **157,** 1216-1229.

Staley K. (2015) Molecular mechanisms of epilepsy. *Nat. Neurosci.* **18,** 367-372.

Sun Q. and Turrigiano G. G. (2011) PSD-95 and PSD-93 play critical but distinct roles in synaptic scaling up and down. *J Neurosci* **31,** 6800-6808.

Sun X. and Lin Y. (2016) Npas4: Linking Neuronal Activity to Memory. *Trends Neurosci.* **39,** 264-275.

Sun X. D., Li L., Liu F. et al. (2016) Lrp4 in astrocytes modulates glutamatergic transmission. *Nat. Neurosci.* **19,** 1010-1018.

Tan G. H., Liu Y. Y., Hu X. L., Yin D. M., Mei L. and Xiong Z. Q. (2011) Neuregulin 1 represses limbic epileptogenesis through ErbB4 in parvalbumin-expressing interneurons. *Nat. Neurosci.* **15,** 258-266.

Turrigiano G. (2011) Too many cooks? Intrinsic and synaptic homeostatic mechanisms in cortical circuit refinement. *Annu Rev Neurosci* **34,** 89-103.

Turrigiano G. G., et al. (2008) The self-tuning neuron: synaptic scaling of excitatory synapses. *Cell* **135,** 422-435.

Ullah I., Badshah H., Naseer M. I., Lee H. Y. and Kim M. O. (2015) Thymoquinone and vitamin C attenuates pentylenetetrazole-induced seizures via activation of GABAB1 receptor in adult rats cortex and hippocampus. *Neuromolecular Med.* **17,** 35-46.

Ye L., Allen W. E., Thompson K. R. et al. (2016) Wiring and Molecular Features of Prefrontal Ensembles Representing Distinct Experiences. *Cell* **165,** 1776-1788.

Yoshihara S., Takahashi H., Nishimura N. et al. (2014) Npas4 regulates Mdm2 and thus Dcx in experience-dependent dendritic spine development of newborn olfactory bulb interneurons. *Cell Rep.* **8,** 843-857.

Yun J., Koike H., Ibi D. et al. (2010) Chronic restraint stress impairs neurogenesis and hippocampus-dependent fear memory in mice: possible involvement of a brain-specific transcription factor Npas4. *J. Neurochem.* **114,** 1840-1851.

## Figure legends

**Figure 1. Homeostatic control of kindling epileptogenesis by Npas4**

**(a, b)** PTZ-induced kindling development in C57BL/6 mice. **(a)** Experimental schedule. **(b)** Seizure score. **(c, d)** *cFos* and *Npas4* mRNA levels in the hippocampus after the single or repeated PTZ treatment. **(c)** Experimental schedule. **(d)** Expression levels of *cFos* and *Npas4* mRNA. **(e)** Rapid development of PTZ-induced kindling in *Npas4* KO mice. **(f)** Potentiation of *cFos* mRNA levels in the hippocampus of *Npas4* KO mice after the repeated treatment with PTZ. Data are presented as the mean±SEM. The n number in the figure indicates number of mice. *p<0.05 and **p<0.01.

**Figure 2. Spatiotemporal expression of Npas4 after convulsive seizures**

**(a)** Experimental schedule. **(b)** Temporal changes in *Npas4* mRNA levels after the PTZ treatment. **(b)** Spatial distribution of *Npas4* mRNA after the PTZ treatment. Scale bars indicate 200 μm. **(c)** Temporal changes in Npas4 and cFos protein levels after the PTZ treatment. **(d)** Spatial distribution of the Npas4 protein after the PTZ treatment. Scale bars indicate 50 μm. Data are presented as the mean±SEM. The n number in the figure indicates number of mice. **p<0.01.

**Figure 3. PTZ stimulates Homer1a expression after convulsive seizure responses**

**(a)** Experimental schedule. **(b)** Temporal changes in *Homer1a* mRNA levels after the PTZ treatment. **(c)** Spatial distribution of *Homer1a* mRNA levels. Scale bars indicate 20 μm. **(d)**

Temporal changes in Homer1a protein levels after the PTZ treatment. **(e)** Spatial distribution of the Homer1a protein after the PTZ treatment. Representative photographs show coronal sections in the CA3 region of the hippocampus. Scale bars indicate 50 μm. Data are presented as the mean±SEM. The n number in the figure indicates number of mice. **p<0.01.

**Figure 4. Npas4 mediates PTZ-induced Homer1a expression in the hippocampus**

**(a-c)** Effects of Npas4 on Home1a promoter activity. **(a)** Experimental schedule. **(b)** Home1a promoter activity with or without the *Npas4* plasmid. **(b)** Mapping of the Npas4 responsive element in the *Homer1a* promoter. The upper panel shows a schematic presentation of the *Homer1a* promoter with 4 different types of putative Npas4 responsive elements (#1−#4). The lower panel shows the relative luciferase activity of the *Homer1a* promoter with different types of putative Npas4 responsive element mutants. **(d-g)** Homer1a levels in the hippocampus of *Npas4* KO mice after the PTZ injection. **(d)** Experimental schedule. **(e)** *Homer1a* mRNA levels. **(f)** Homer1a protein levels. **(g)** Co-localization of *Homer1a* mRNA with the Npas4 protein after the PTZ treatment. Representative photographs show coronal sections in the CA3 region of the hippocampus. Scale bars indicate 20 μm. The n number in the figure indicates number of wells (b, c) or mice (e, f). Data are presented as the mean±SEM. **p<0.01.

**Figure 5. Npas4 adapts homeostatic scaling though surface AMPAR expression after convulsive seizure responses**

**(a)** Experimental schedule. **(b)** Temporal changes in surface AMPAR GluA1 subunit levels in the hippocampus of PTZ-treated mice. **(c)** Surface AMPAR GluA1 subunit levels in the hippocampus of PTZ-treated *Npas4* KO mice. **(d)** The strength of synaptic transmission evoked at AC-CA3 synapses in wild-type and *Npas4* KO mice 24 h after the PTZ treatment. The left panel shows typical recordings of fEPSPs evoked at AC-CA3 synapses. Quantification of the fEPSP/PSFV ratio is shown in the right panel. **(e)** mEPSCs in hippocampal CA3 neurons of wild-type and *Npas4* KO mice 24 h after the PTZ treatment. The left panel shows typical recordings of mEPSCs. Quantification of the average amplitude of mEPSCs is shown in the right panel. Data are presented as the mean±SEM. The n number in the figure indicates number of mice (b, c) or slices (d, e). *p<0.05 and **p<0.01.

**Figure 6. Npas4 controls homeostatic scaling during kindling development though Homer1a**

**(a)** Experimental schedule. **(b)** Schematic of AAV-mediated Homer1a expression in the hippocampus. Representative coronal brain slices showing the expression of EGFP 3 weeks after the AAV injection into the hippocampus. The scale bar represents 200 μm. **(c)** Confocal images of AAV-injected mice. The scale bar indicates 50 μm. **(d)** Reductions in surface AMPAR GluA1 subunit levels in the hippocampus of AAV-*Homer1a*-microinjeted *Npas4* KO mice. **(e)** Suppression of PTZ-induced kindling development in AAV-*Homer1a*-microinjeted *Npas4* KO mice. Data are presented as the mean±SEM. The n number in the figure indicates number of mice. *p<0.05 and **p<0.01.

Figure 1

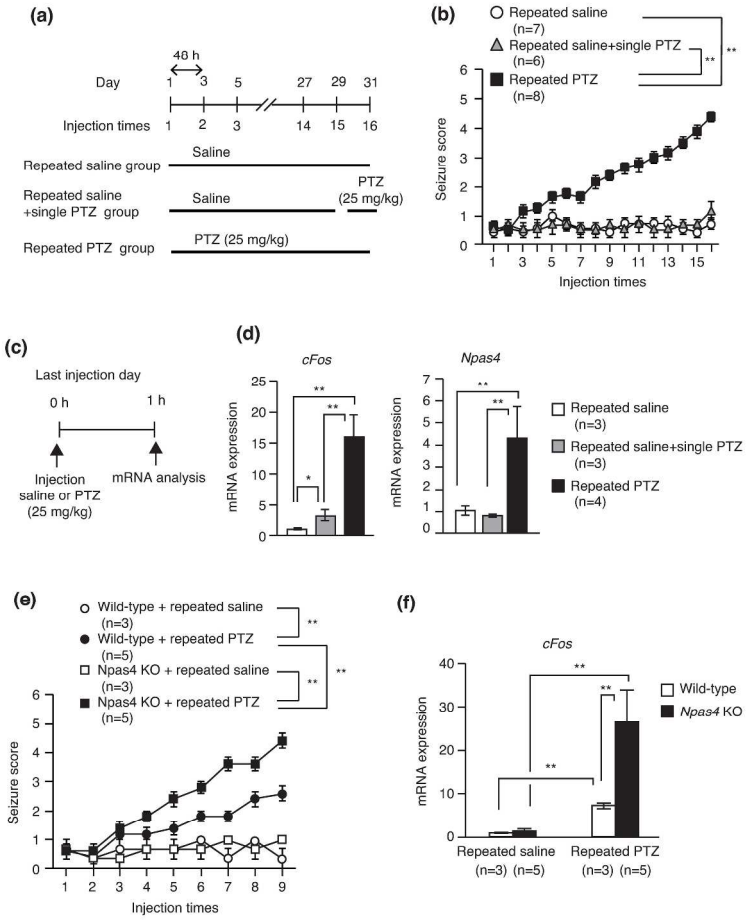


Fig. 1

309x384mm (300 x 300 DPI)

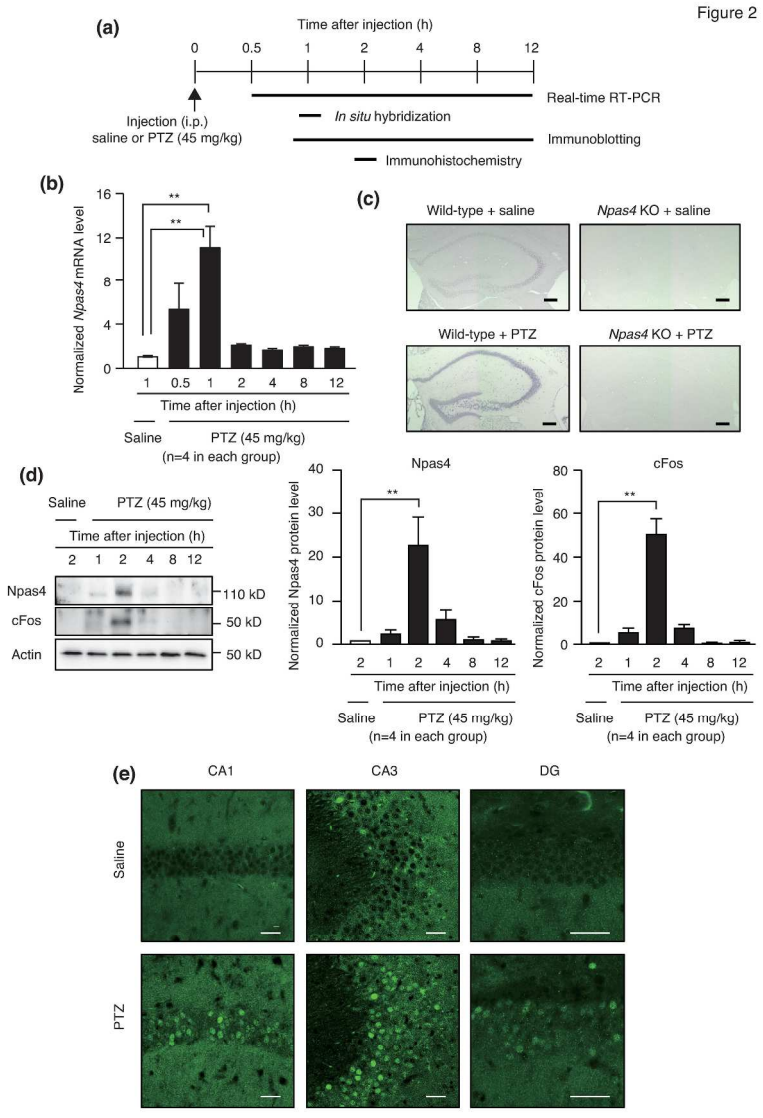


Fig. 2

309x384mm (300 x 300 DPI)

Figure 3

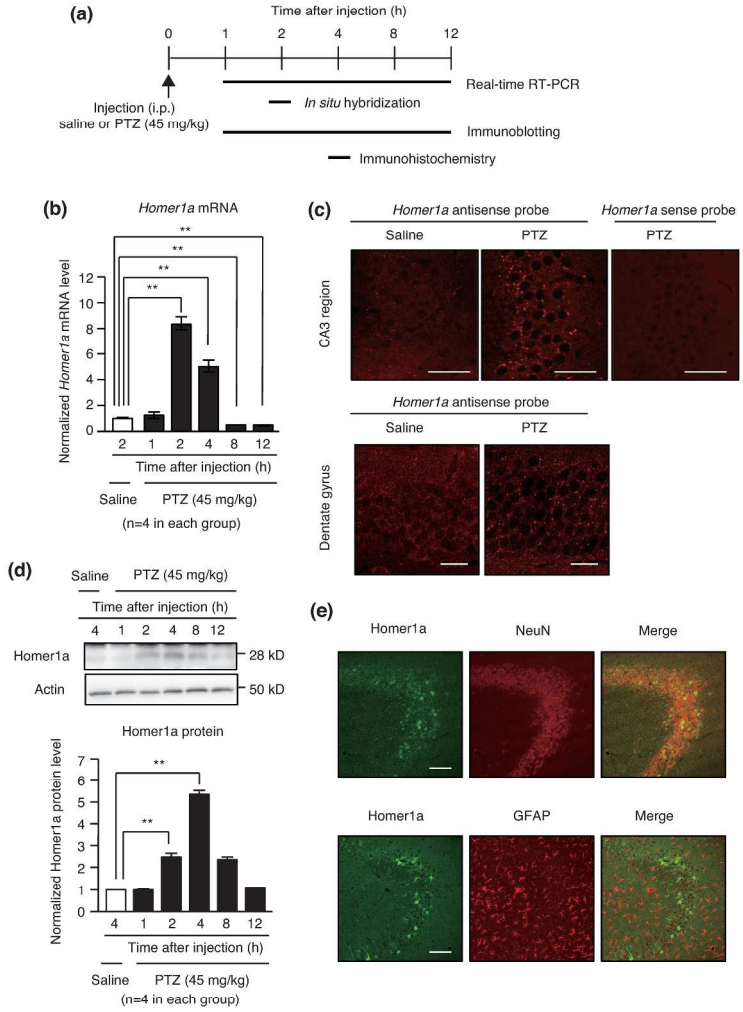


Fig. 3

309x384mm (300 x 300 DPI)

Figure 4

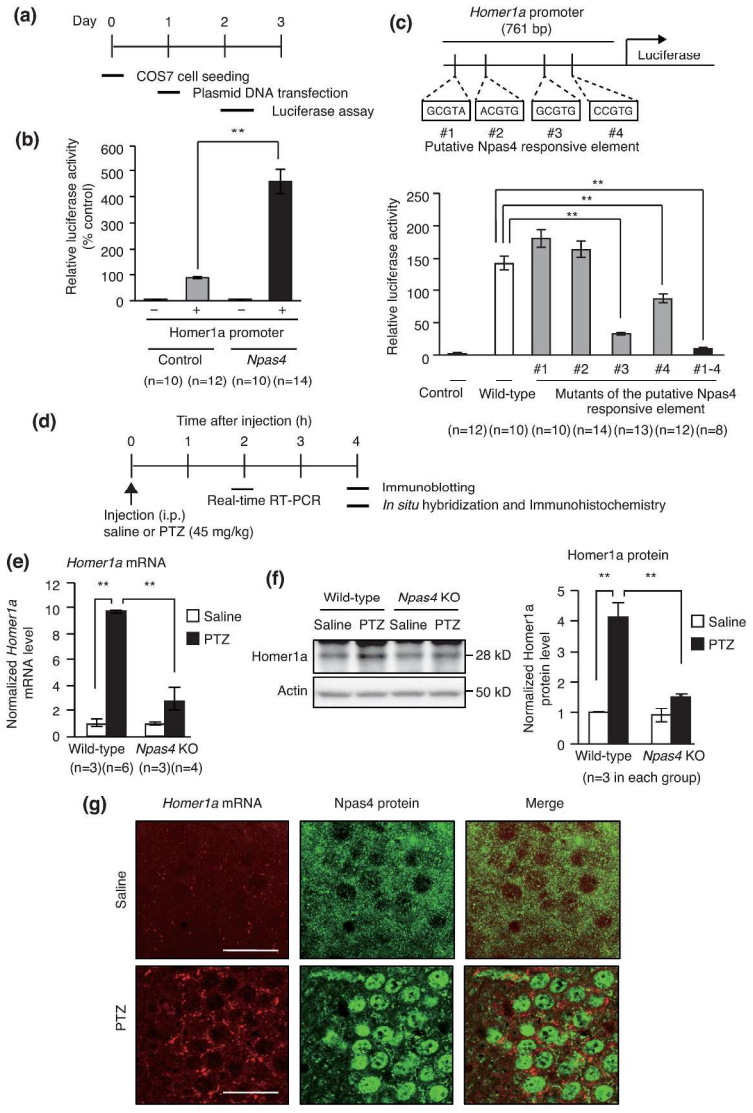


Fig. 4

309x384mm (300 x 300 DPI)

Figure 5

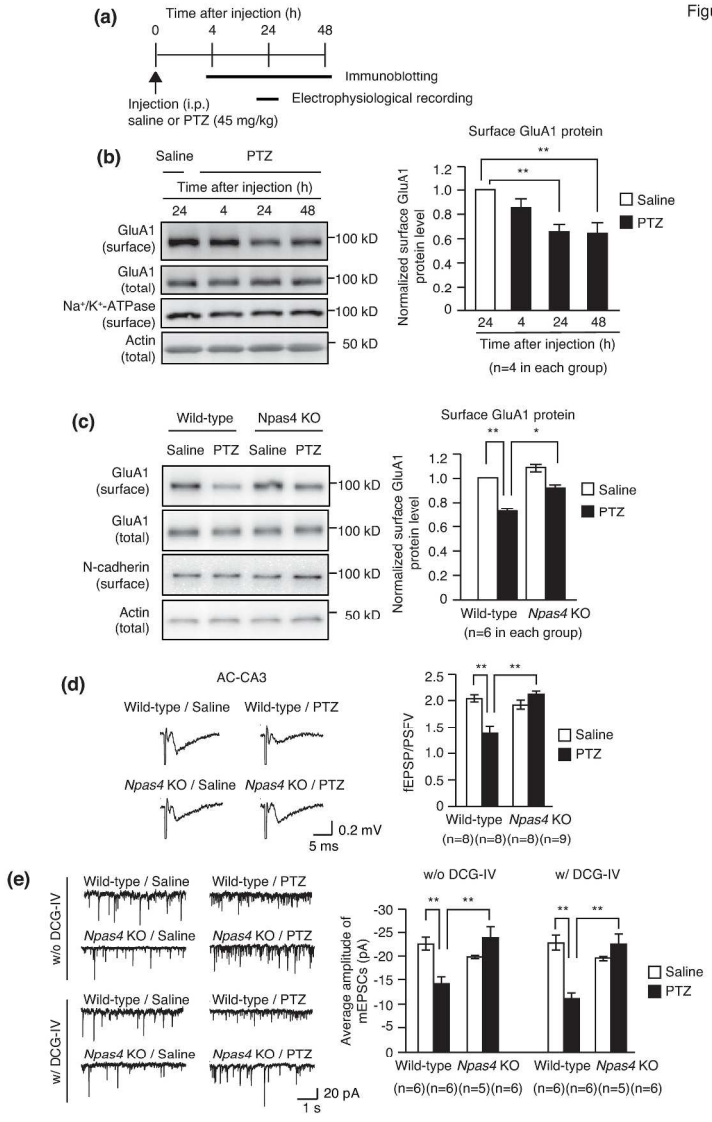


Fig. 5

309x384mm (300 x 300 DPI)

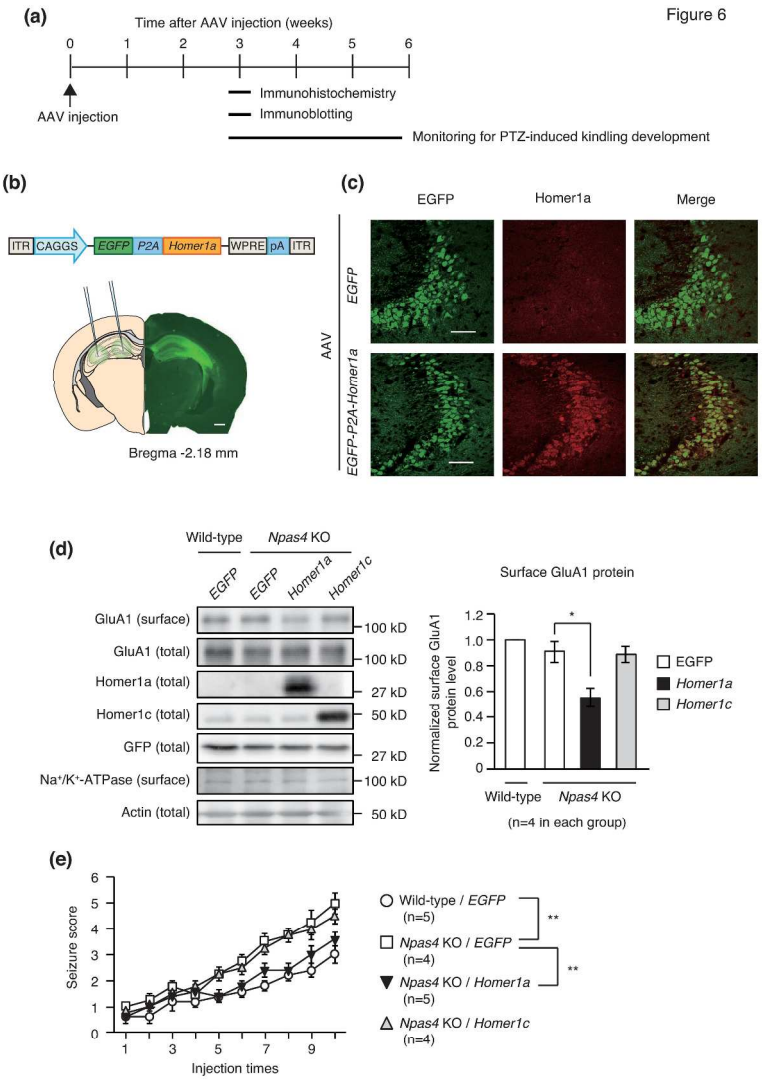


Fig. 6

309x384mm (300 x 300 DPI)

# Neuronal PAS domain protein 4 (Npas4) controls neuronal homeostasis in pentylenetetrazole-induced epilepsy through the induction of Homer1a

Wei Shan, Taku Nagai, Motoki Tanaka, Norimichi Itoh, Yoko Furukawa-Hibi, Toshitaka Nabeshima, Masahiro Sokabe, Kiyofumi Yamada

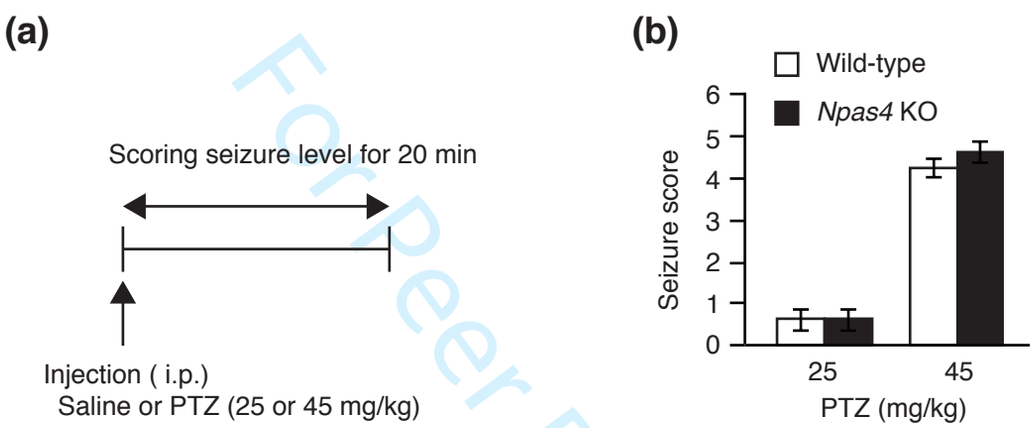




**Supplementary Figure S1. Effects of a single treatment with PTZ on convulsive seizures**

**(a)** Experimental schedule. Mice were administered PTZ (25 or 45 mg/kg, i.p.) and their behaviors were monitored for 20 min after the injection. **(b)** Effect of PTZ on convulsive seizures in wild-type and *Npas4* KO mice. Data are presented as the mean±SEM (number of mice in each group, n=5). A two-way ANOVA analysis; genotype, $F(1,16)=0.73$, $p=0.41$; PTZ treatment, $F(1,16)=262.50$, $p<0.01$; interaction, $F(1,16)=0.73$, $p=0.41$.

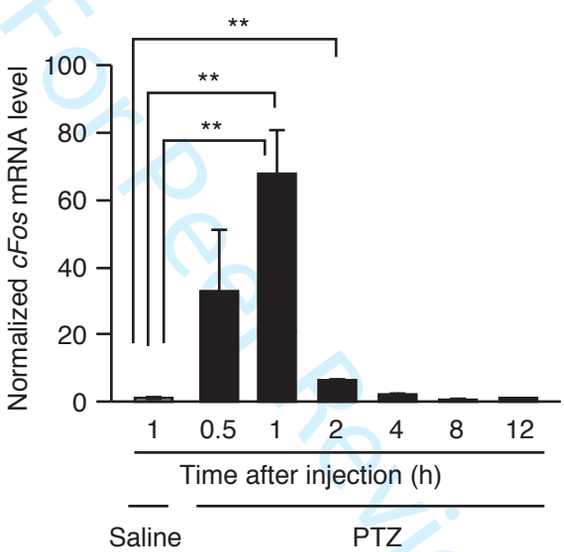


**Supplementary Figure S2. Temporal changes in cFos mRNA levels after the PTZ treatment** C57BL/6 mice were administered saline or PTZ (45 mg/kg), and *cFos* mRNA levels in the hippocampus were measured after the injection. Data are presented as the mean±SEM (number of mice in each group, n=4). An one-way ANOVA analysis; $F(6, 21)=86.72$, $p<0.01$. **$p<0.01$.

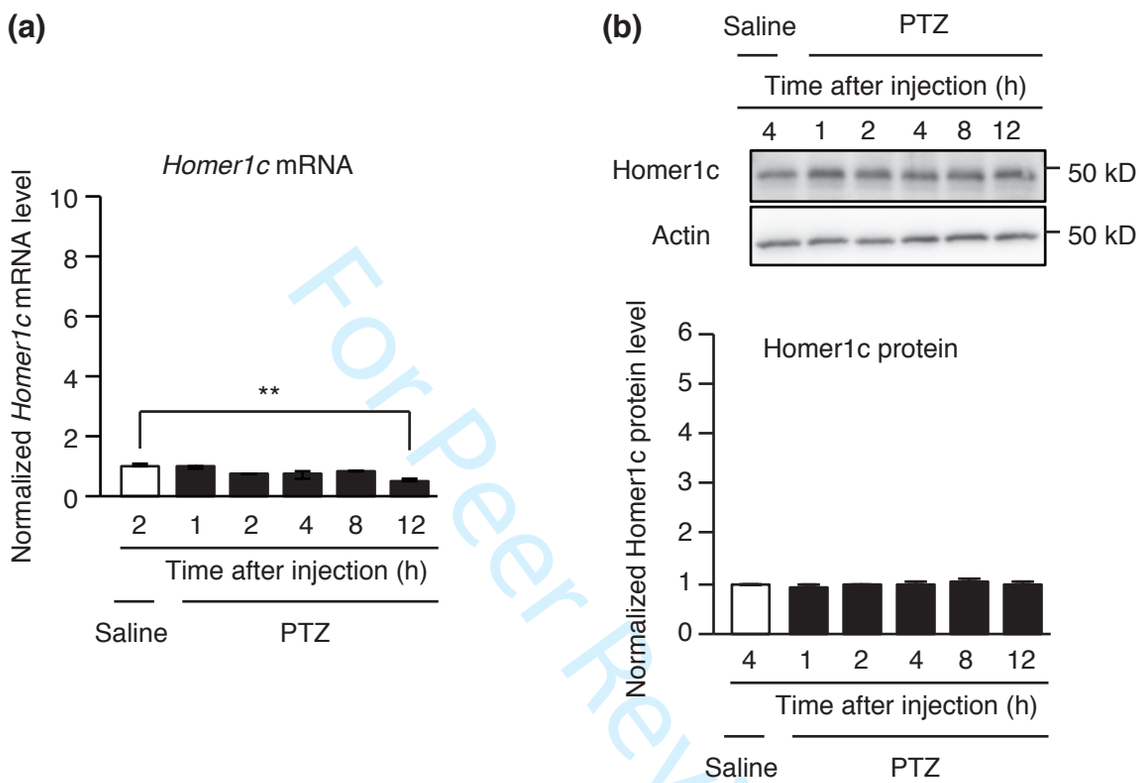




**Supplementary Figure S3. Homer1c expression after the PTZ treatment**
**(a)** Temporal changes in *Homer1c* mRNA levels after the PTZ treatment. C57BL/6 mice were administered saline or PTZ (45 mg/kg), and *Homer1c* mRNA levels in the hippocampus were measured after the injection. Data are presented as the mean±SEM (number of mice in each group, n=4). An one-way ANOVA analysis; $F(5,18)=7.689$, $p<0.01$. **$p<0.01$. **(b)** Temporal changes in Homer1c protein levels after the PTZ treatment. Upper panels show immunoblots for Homer1c. Quantification of the immunoblotting assay is shown in the bottom panel. Data are presented as the mean±SEM (number of mice in each group, n=4). An one-way ANOVA analysis; $F(5,18)=0.38$, $p=0.86$.

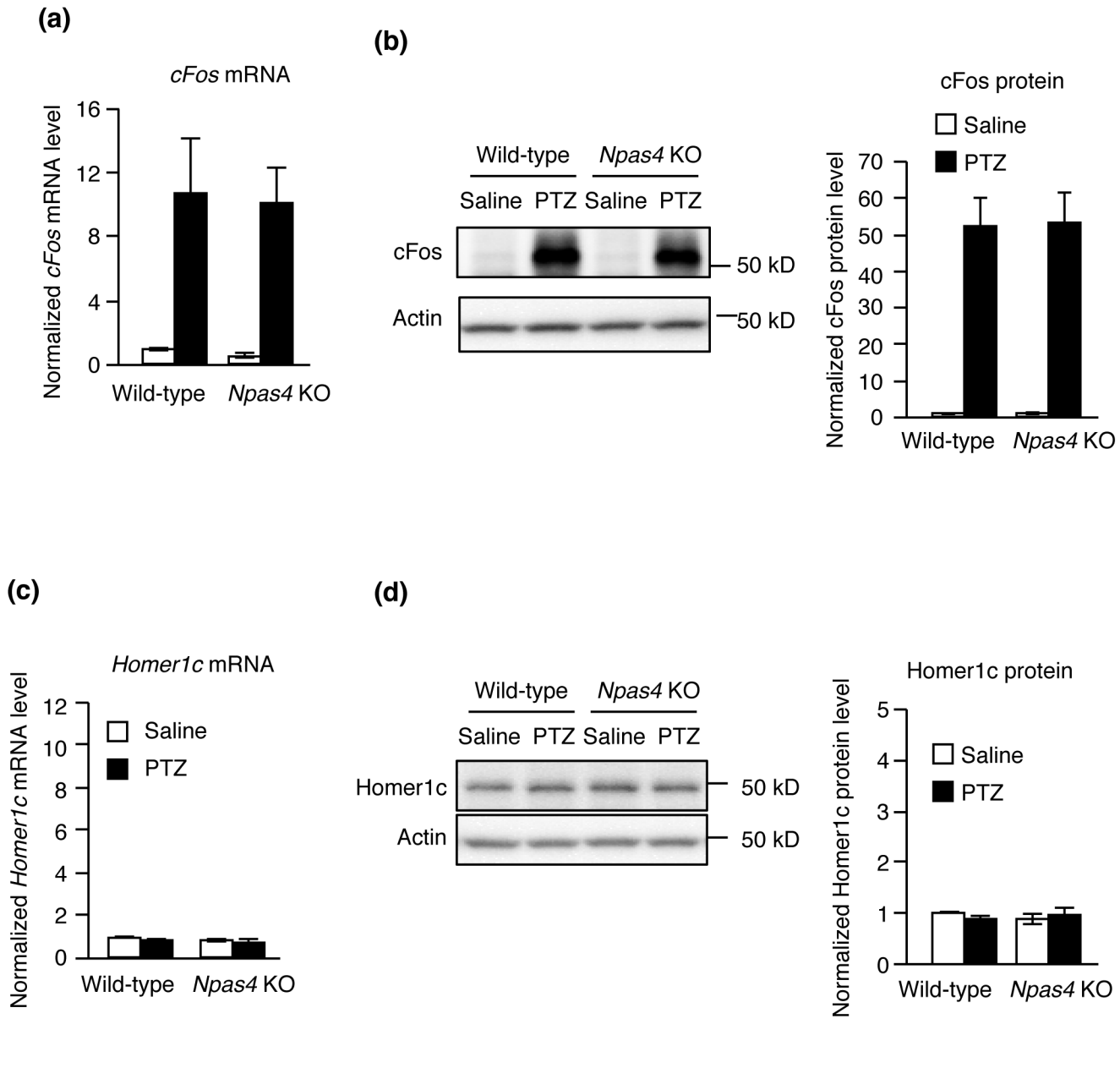


**Supplementary Figure S4. Effects of PTZ on cFos and Homer1c expression in *Npas4* KO mice**

**(a)** Effects of PTZ on *cFos* mRNA expression. *cFos* mRNA levels in the hippocampus were measured 1 h after the PTZ injection. Data are presented as the mean±SEM (number of mice in each group, n=4). A two-way ANOVA analysis; genotype, $F(1,12)=2.67$, $p=0.13$; PTZ treatment, $F(1,12)=81.52$, $p<0.01$; interaction, $F(1,12)= 2.469$, $p=0.14$. **(b)** Effects of PTZ on cFos protein expression. cFos protein levels in the hippocampus were measured 2 h after the PTZ injection. Data are presented as the mean±SEM (number of mice in each group, n=3). A two-way ANOVA analysis; genotype, $F(1,8)=0.01$, $p=0.91$; PTZ treatment, $F(1,8)=88.02$, $p<0.01$; interaction, $F(1,8)=0.01$, $p=0.92$. **(c)** Effects of PTZ on *Homer1c* mRNA expression. *Homer1c* mRNA levels in the hippocampus were measured 2 h after the PTZ injection. Data are presented as the mean±SEM (number of mice; n=3 for saline-treated wild-type, n=6 for PTZ-treated wild-type, n=3 for saline-treated Npas4 KO, n=4 for PTZ-treated Npas4 KO). A two-way ANOVA analysis; genotype, $F(1,12)=0.3571$, $p=0.56$; PTZ treatment, $F(1,12)=1.33$, $P=0.27$; interaction, $F(1, 12)=1.985$, $p=0.18$. **(d)** Effects of PTZ on Homer1c protein expression. Homer1c protein levels in the hippocampus were measured 4 h after the PTZ injection. Data are presented as the mean±SEM (number of mice in each group; n=3). A two-way ANOVA analysis; genotype, $F(1,8)=0.03$, $P=0.87$; PTZ treatment, $F(1,8)=0.08$, $p=0.78$; interaction, $F(1,8)=2.42$, $P=0.16$.

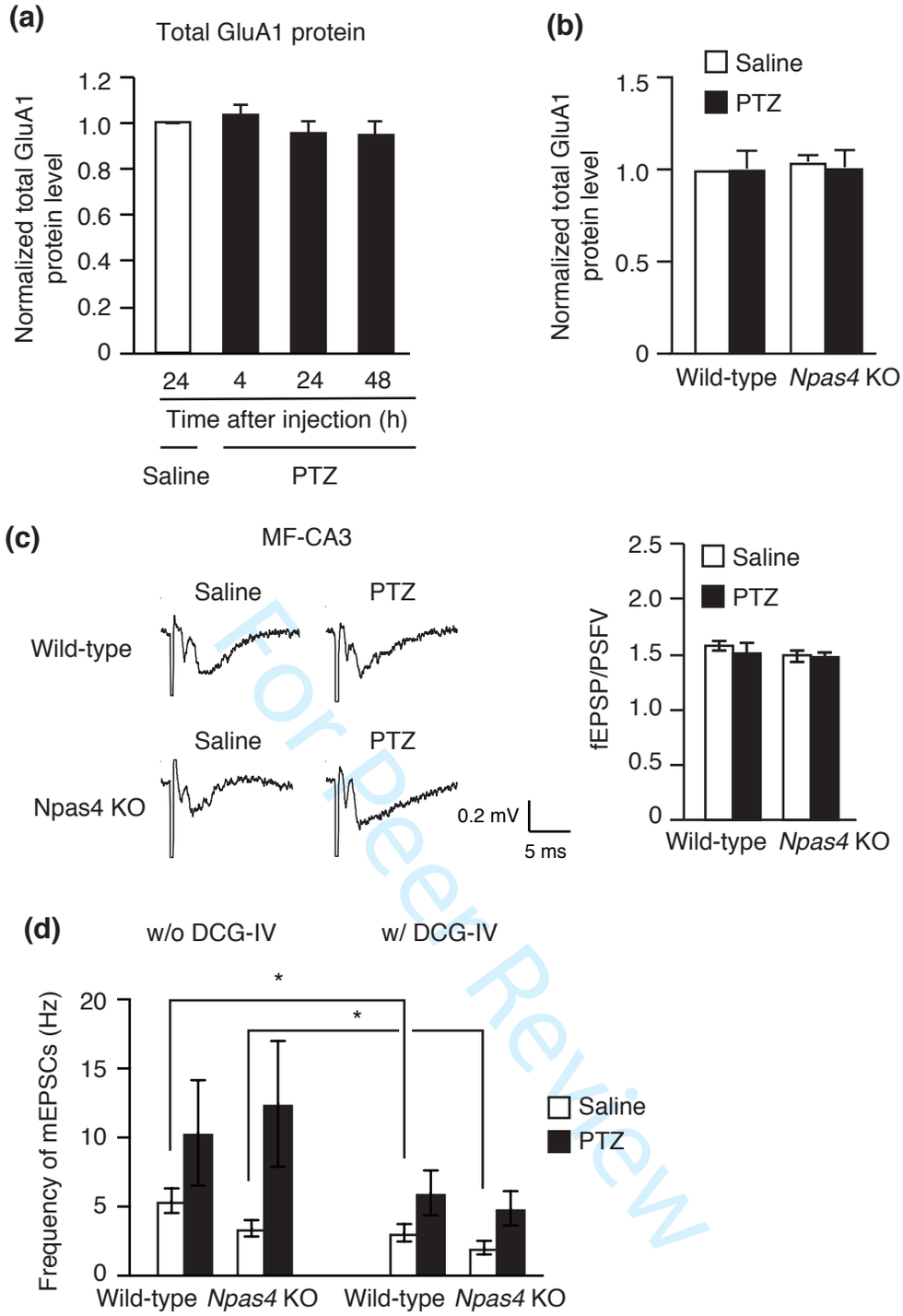




**Supplementary Figure S5. Effects of PTZ on excitatory synaptic transmission in *Npas4* KO mice**

**(a)** Temporal changes in total AMPAR GluA1 subunit levels in the hippocampus of PTZ-treated mice. Total AMPAR GluA1 subunit levels in the hippocampus were measured after the PTZ injection. Data are presented as the mean±SEM (number of mice in each group, n=4). A one-way ANOVA analysis; F(3,12)=0.86, p=0.49. **(b)** Total AMPAR GluA1 subunit levels in the hippocampus of PTZ-treated *Npas4* KO mice. Total AMPAR GluA1 subunit levels in the hippocampus were measured 24 h after the PTZ injection. Data are presented as the mean±SEM (number of mice in each group, n=4). A two-way ANOVA analysis; genotype, F(1,12)=0.12, p=0.73; PTZ treatment, F(1,12)=0.03, p=0.86; interaction, F(1,12)=0.06, p=0.82. **(c)** Strength of evoked synaptic transmission at MF-CA3 synapses in wild-type and *Npas4* KO mice 24 h after the PTZ treatment. The left panel shows typical recordings of fEPSPs evoked at MF-CA3 synapses in saline- and PTZ-treated wild-type and *Npas4* KO mice. Quantification of the fEPSP/PSFV ratio is shown in the right panel. Data are presented as the mean±SEM (number of slice in each group; n=8 for saline-treated wild-type, n=7 for PTZ-treated wild-type, n=9 for saline-treated *Npas4* KO, n=8 for PTZ-treated *Npas4* KO). A two-way ANOVA analysis; genotype, F(1,28)=0.96, p=0.34; PTZ treatment, F(1,28)=0.43, p=0.52; interaction, F(1,28)=0.29, p=0.59. **(d)** Frequency of mEPSCs in the hippocampal CA3 neurons of wild-type and *Npas4* KO mice 24 h after the PTZ treatment. Data are presented as the mean±SEM (number of slice in each group; n=6 for saline-treated wild-type, n=6 for PTZ-treated wild-type, n=5 for saline-treated *Npas4* KO, n=6 for PTZ-treated *Npas4* KO). A three-way ANOVA analysis; genotype, F(1,38)=0.10, p=0.76; PTZ treatment, F(1,38)=8.55, p<0.01; DCG-IV treatment, F(1,38)=5.38, p<0.05; genotype×PTZ interaction, F(1,38)=0.37, p=0.55; PTZ treatment×DCG-IV treatment interaction, F(1,38)=1.49, p=0.23; genotype×PTZ treatment×DCG-IV treatment interaction, F(1,38)=0.38, p=0.54. *p<0.05.

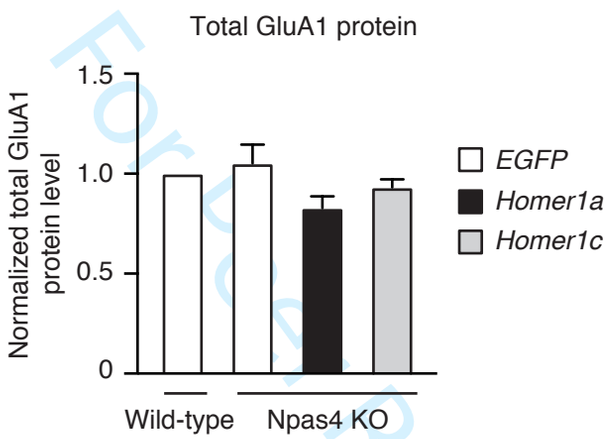


**Supplementary Figure S6. Total AMPA GluA1 subunit levels in the hippocampus of AAV-Homer1a and Homer1c-microinjected *Npas4* KO mice**

Data are presented as the mean±SEM (number of mice in each group, n=4). An one-way ANOVA analysis; F(2,9)=2.721, p=0.12.

| MS number | Full Paper | Date received |
|---|---|---|
| JNC-2017-0640.R1 | Full paper | 18/10/17 |

| Special issue / comments |
|---|
| |

| All authors |
|---|
| Yamada, Kiyofumi (contact); shan, wei; Nagai, Taku; Tanaka, Motoki; Itoh, Norimichi; Furukawa-Hibi, Yoko; Nabeshima, Toshitaka; Sokabe, Masahiro |

| Title |
|---|
| Neuronal PAS domain protein 4 (Npas4) controls neuronal homeostasis in pentylenetetrazole-induced epilepsy through the induction of Homer1a |

| Corresponding author |
|---|
| Prof. Kiyofumi Yamada |

| Address |
|---|
| |

| Tel |
|---|
| |

| FAX |
|---|
| |

| E-mail |
|---|
| kyamada@med.nagoya-u.ac.jp |

| Date of first decision | Date received 1st revision | Date received 2nd and further revisions |
|---|---|---|
| 17/11/17 | 27/11/17 | |

| Final Decision | Days to 1st decision | Days submission to final decision |
|---|---|---|
| Accepted on 28/11/17 | 29 | 31 |

| Copyright Form | Disk Enclosed | Colour Figures |
|---|---|---|
| No | N/A | |

| ISN member - Confirmation | Category |
|---|---|
| No | Signal Transduction & Synaptic Transmission |

We investigated the mechanism by which neuronal PAS domain protein 4 (Npas4) regulates epilepsy using pentylenetetrazol (PTZ)-treated mice. PTZ treatment increased excitatory inputs followed by Npas4 induction in the hippocampus. Npas4 controlled the surface expression of the α-amino-3-hydroxy-5-methyl-4-isoxazole propionic acid-type glutamate receptor (AMPAR) through the introduction of Homer1a. We propose that Npas4 functions as a molecular switch to initiate homeostatic scaling in epilepsy.

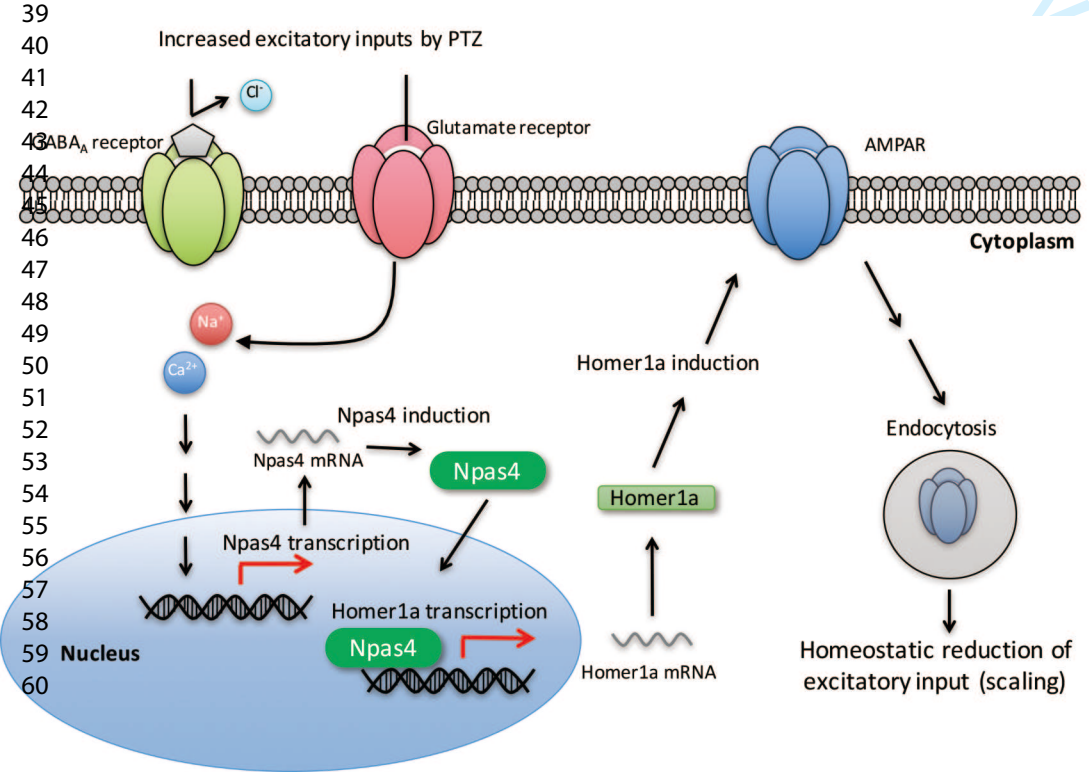

**Data Reporting Checklist**

Animal studies based on ARRIVE guidelines (https://www.nc3rs.org.uk/arrive-guidelines)

*If any item is not applicable, indicate "n/a" and the reason why it is not applicable!*

| Checklist item | Description | Reported on page number |
|---|---|---|
| **Ethical statement** | - Institutional approval (name of institution and reference number) | - P7 |
| **Study design** | **Pre-registration of the study**<br>- Statement if/where study was pre-registered | No, our institution does not required. P7 |
| | **Randomization (mandatory for all animal experiments)**<br>- Full details of how animals were allocated to experimental groups | - P7, 37-39, Figures |
| | - Randomization method (randomization table, computer based randomization, etc.) | - P8 |
| | - Order in which animals were treated and assessed | - P7-8 |
| | - Statement if no randomization was performed | - n/a |
| | **Blinding**<br>- Who was blinded (experimenter, person assigning subjects to groups, etc.) | - P8 |
| | - When (at which point in the experimental course) | - P8 |
| | - How (describe blinding procedure) | - P8 |
| | - Statement if no blinding was performed | - n/a |
| | **Predetermined sample size calculation (mandatory for animal studies)**<br>- Statement whether statistical methods were used to predetermine sample size and description of the calculation | - P16 |
| | **Outcomes**<br>- Pre-specified primary or secondary endpoint, otherwise exploratory | - P7-16 |
| | - Predefined criteria how to deal with outliers | - P7-16 |
| | **Provide time-line diagram or flow-chart (mandatory for animal experiments)** | - P7, P16-25, Figures |
| | **At the end of study report**<br>- Information on replication [*biological* (independent data points from different sources) or *technical replicates* (repetition of the assay/sample preparation from the same source)] | - P16-25, P37-39 |
| | - Definition of Sample size (n): Report exact numbers for all experiments (figures) | - P16-25, P37-39 |
| | - Explanation of any sample size differences between beginning and end for each experiment | - P16 |
| | **Data availability**<br>- Mandatory for: Protein, DNA and RNA sequences, Macromolecular structures, crystallographic data for small molecules, microarray data (*strongly recommended for all* | - P7-25 |

| Checklist item | Description | Reported on page number |
|---|---|---|
| | *other data sets*)<br>- Weblink to repository / accession codes / other unique identifiers<br>- Computer code availability<br>- Statement to any restrictions on the availability of materials/data<br>- Raw western blot or electrophoresis images provided as supplement material? (Yes/No) | <br>- P7-16<br>- n/a<br>- n/a<br>- No |
| **Experimental procedure** | **Precise details of all procedures carried out:**<br>- What (Materials such as antibodies, reagents with Research Resource Identifiers ((RRIDs) from https://scicrunch.org)<br>- Antibodies: validation data available from the company or conducted by the authors<br>- How (drug formulation; dose, site and route, anesthesia/analgesia, surgical procedure, method of euthanasia, details about specialist equipment incl. suppliers)<br>- When (e.g. time of day).<br>- Where (e.g. home cage, laboratory, water maze).<br>- Why (e.g. rationale for choice of specific anesthetic, route of administration, drug dose used) | <br>-P7-16<br>-P7-16<br>- P7-16<br>- P8<br>- P8<br>- P7-16 |
| **Animals/ Cell lines** | - Species, strain<br>- Source of animals / cell lines (indicate provider, catalog number, RRID from https://scicrunch.org)<br>- State if and when animals or cell lines were last authenticated<br>- Statement if cell line is listed as a commonly misidentified cell line by the International Cell Line Authentication Committee (ICLAC; http://iclac.org/databases/cross-contaminations/)<br>o If the cell line is listed, provide a scientific justification to use this cell line<br>- Sex<br>- Age<br>- Weight<br>- Housing (type of cage, number of cage companions)<br>- Husbandry (access to food and water, light/dark cycle, temperature, environmental enrichment)<br>- Welfare-related assessments and interventions | - P7, 12<br>- P7, 12<br>- P7,12<br>- n/a<br>- P7<br>- P7<br>- P7<br>- P7<br>- P7<br>- P7 |
| **Reporting statistics** | **Describe the statistical tests that were used and why these tests were chosen**<br>- Details of the statistical methods used for each analysis<br>- Specify the unit of analysis (n) for each dataset (e.g. single animal, group of animals, single neuron)<br>- Describe any methods used to<br>o assess whether the data met the assumptions of the statistical approach<br>o to control for confounding<br>o examine subgroups and interactions<br>- Explain how missing data were addressed<br>- Provide exact p-values<br>- Correction for risk of false positives in case of multiple testing | <br>- P16-25<br>- P37-39<br>-<br>- P16-25<br>- P16-25<br>- P16-25<br>- P16-25<br>- P16-25<br>- P16-25 |